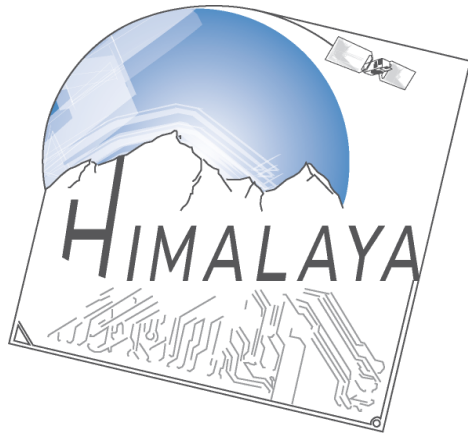| Publication Year	2010
Acceptance in OA@INAF	2024-01-23T16:57:51Z
Title	High performance Mass market GNSS receiver muLTi standard ready for mArket - Advanced Antenna Core Technology Report
Authors	NALDI, Giovanni; MONTEBUGNOLI, STELIO; Iera, Christian; Moriggia, Lorenzo
Handle	http://hdl.handle.net/20.500.12386/34603
Number	WP3 - D3.6

HIMALAYA

D3.6

Advanced Antenna Core Technology Report

File:	HIMA-D36-WP3-INAF-013-310810.doc
Version:	1.3
Release Date:	31/08/2010
By:	Giovanni Naldi (RTM), Stelio Montebugnoli (RTM), Christian Iera (EXYS), Lorenzo Moriggia (EXYS)
Permissions:	Public

FP7-GALILEO-2007-GSA-1

High performance Mass market GNSS receiver muLTi standard ready for mArket

228430

HIMALAYA Project

Advanced Antenna Core Technology Report

Date of preparation: 31 August 2010

Version number: 1.3

Dissemination level: PU

List of contributors

Beneficiary no.	Organization name	Short name	Country	Effort spent (pm)
1	Radioastronomy Institute of Medicina	RTM	Italy	3.8
2	ECLEXYS SAGL	EXYS	Switzerland	

Revision History

Revision	Date	By:	Description
1.0	23 February 2010	Giovanni Naldi (RTM), Stelio Montebugnoli (RTM)	First version of the document
1.1	26 February 2010	Giovanni Naldi (RTM)	Second version of the document
1.2	17 August 2010	Giovanni Naldi (RTM), Stelio Montebugnoli (RTM)	Final version of the document
1.3	31 August 2010	Christian Iera (EXYS), Lorenzo Moriggia (EXYS), Damien Kubrak (TAS-F)	EXYS: contribution on Chapter 2 (*GNSS Antennas*) and revision of the final version of the document. TAS-F: revision of the final version of the document.

Abstract

This HIMALAYA Deliverable, "D3.6 Advanced Antenna Core Technology Report", is focused on the preliminary study of an antenna design solution that can provide multi-frequency functionality to mobile phones, with the intent of reducing costs and improving performances with respect to the existing systems.

The first chapter of this document presents an introduction on the general characteristics and requirements for the better antenna implementation.

In the second chapter there is an overview of the most used antennas in modern cellular phones, with good and bad qualities for each of them.

The third chapter considers the most important problems connected to the combined antennas for mobile phones; in other words it's about all the problems that arise from the integration of several services in a very small device.

In the fourth chapter it is reported a benchmarking study that compares the performances of some GPS antennas working on commercial handsets. This activity is fully described in a document of Sagem Wireless. The results that came out of this study are useful to benchmark the choices for the Himalaya receiver.

The fifth chapter provides a preliminary multi-frequency antenna design study intended for a mobile device with GPS, GSM1800, UMTS and WLAN/Bluetooth functionalities.

In the sixth chapter it is presented a general overview on beam-forming methods applicable to devices equipped with an array of receivers.

The conclusions are reported in the seventh chapter.

Table of Contents

Table of Figures

Table of Tables

1. Introduction

1.1. Acronyms

AR	Axial Ratio
AM	Amplitude Modulation
BT	Bluetooth
CDMA	Code Division Multiple Access
CW	Continuous Wave
dB	Decibel
dBi	Decibels relative to an isotropic antenna
DDC	Digital Down Converter
DOA	Direction Of Arrival
DRA	Dielectric Resonator Antenna
EBG	Electromagnetic Band-Gap
FEA	Fractal Element Antenna
FM	Frequency Modulation
FR 4	Flame Retardant 4
GNSS	Global Navigation Satellite Systems
GPRS	General Packet Radio Service
GPS	Global positioning system
GSM	Global System for Mobile communications
IFA	Inverted F Antenna
IMT2000	International Mobile Telecommunications-2000
L1	GPS-L1
L2	GPS-L2
L5	GPS-L5
LCMV	Linearly Constrained Minimum Variance
LHCP	Left handed circular polarization

LNA	Low Noise Amplifier
MSC	Multiple Sidelobe Canceller
PCB	Printed Circuit Board
PEC	Perfect Electric Conductor
PIFA	Planar Inverted F Antenna
RHCP	Right handed circular polarization
RF	Radio Frequency
SBAS	Satellite Based Augmentation System
SINR	Signal to Interference plus Noise Ratio
SNR	Signal to Noise Ratio
SWR	Standing Wave Ratio
UMTS	Universal Mobile Telecommunications System
VSWR	Voltage Standing Wave Ratio
Wi-Fi	Wireless Fidelity
WLAN	Wireless Local Area Network

1.2. References

Ref.	Description
[1]	Constantine A. Balanis. "*Antenna Theory: Analysis and Design, 3rd Edition*"
[2]	Warren L. Stutzman. "*Antenna Theory and Design, 2nd Edition*"
[3]	K. L. Wong. "*Planar Antennas for Wireless Communications*". Published by John Wiley & Sons, New York, 2003
[4]	Y.X. Guo, M.Y.W. Chia, and Z.N. Chen. "*Miniature Built-in Multiband Antennas for Mobile Handsets*". Published in IEEE Transactions on Antennas and Propagation, Vol. 52, No. 8, August 2004, pp. 1936–1944 (doi: 10.1109/TAP.2004.832375).
[5]	M. John, M. J. Ammann and R. Farrell. "*Printed Triband Terminal Antenna*". Centre for Telecommunications Value-chain driven Research
[6]	Heng Deng, Zhenghe Feng. "*A Triple-Band Compact Monopole Antenna for Mobile Handsets*". Department of electronic engineering Tsinghua University, Beijing, China
[7]	B. Rama Rao, E. N. Rosario, Mohamed S. Mahmoud, Jay I. Simon. "*Compact Co-Planar Dual-Band Microstrip Patch Antennas for Modernized GPS*". The MITRE Corporation,, Bedford, Massachusetts.

[8]	S.A. Long, M.W. McAllister and L.C. Shen. "*The Resonant Cylindrical Dielectric Cavity Antenna*". IEEE Transactions On Antennas and Propagation, AP-31, pp. 406-412, 1983.
[9]	R.K. Mongia and P. Bhartia. "*Dielectric Resonator Antennas—A Review and General Design Relations for Resonant Frequency and Bandwidth*". International Journal of Circle 15 or visit freeproductinfo.net/rfd Microwave and Millimeter-Wave Computer- Aided Engineering, 4, (3), pp. 230-247, 1994
[10]	Z. Wang, C. C. Chiau, X. Chen, B. S. Collins, S. P. Kingsley and S. Puckey. "*Study and Optimisation of a Broadband Dielectric Antenna*". Presented at the IEEE International Workshop on Antenna Technology: Small Antennas and Novel Metamaterials, Singapore, March 7-9, 2005.
[11]	X. L. Bao, G. Ruvio, M. J. Ammann, and M. John. "*A Novel GPS Patch Antenna on a Fractal Hi-Impedance Surface Substrate*". IEEE ANTENNAS AND WIRELESS PROPAGATION LETTERS, VOL. 5, 2006
[12]	Pavel Hazdra, Milo¡s Mazanek. "*The Miniature Fractal Patch Antenna*". Czech Technical University in Prague, Department of Electromagnetic Field
[13]	R. Glogowski and C. Peixeiro, "*Multiple Printed Antennas for Integration Into Small Multistandard Handsets*", IEEE Antennas And Wireless Propagation Letters, Vol, 7, 2008, pp. 632-635
[14]	A. Rennings, S. Otto, A. Pimpertz, P. Waldow , "*A low-profile antenna solution for mobile phones with GSM, UMTS and WLAN operation*", Microwave Conference, 2005 European. 04/11/2005
[15]	H. Halheit, A. V. Vorst, "*A SimpleWideband Antenna for Mobile Handset*", 3rd European Conference on Antennas and Propagation, Berlin, Germany, 03/23/2009 - 03/27/2009, pp.553-555
[16]	Zhan Li and Yahya Rahmat-Samii, "*Optimization of PIFA-IFA Combination in Handset Antenna Designs*", IEEE Transactions On Antennas And Propagation, Vol. 53, NO. 5, MAY 2005, pp. 1770-1778
[17]	A. Chebihi, C. Luxey, A. Diallo, P. Le Thuc, and R. Staraj, "*A Novel Isolation Technique for Closely Spaced PIFAs for UMTS Mobile Phones*", IEEE Antennas And Wireless Propagation Letters, Vol,7, 2008, pp. 665-668
[18]	A. K. Wang and Jonathan Leary, "SMI Based Beamforming Algorithms for TDMA Signals", Applied Signal Technology, Inc., Sunnyvale, CA 94086, E-mail: akw@appsig.com, 0-8186-8316-3/98 $10.00 (c) 1998 IEEE

1.3. Objectives (from Technical Annex)

GNSS Solution for mobile communications are required nowadays to operate integrated within any type of mobiles, with strong constraints on antenna integration (no external antenna, multimode antenna, interference with GSM/UMTS transceiver …).

The advanced antenna techniques planned in this project are basically summarized in the following approaches:

– Multi-band antennas – e.g. GPS, GSM, Bluetooth frequency bands.

– Enhanced performances;

– Reduced costs;

– Integration issues in a mass-market device - e.g. closed mobile phone.

1.4. Description of the work (from Technical Annex)

The antenna design has to face several problems, mainly related to the integration of different antennas, each of them working in a particular bandwidth, in the same platform.

The modern mobile phones implement a vast number of transmit and receive frequencies, modulation types and standards. Of particular concern is the advent of wideband CDMA signals, which can cause intermodulation products appearing in band at the intermediate frequency of the GPS receiver. Special receiver techniques are required in this case, but the antenna is unable to help except by being of naturally narrow bandwidth.

From this point of view, concepts like coexistence and cohabitation assume very high importance.

Coexistence means the ability to share a platform that includes many antennas (transceiver systems) which have to be only marginally affected the ones with the others, whatever they are doing (such as transmitting full power, low power or idling).

Cohabitation describes the isolation between functions of the same device. For example it's necessary to investigate GPS antennas combined with Wi-Fi and Bluetooth services. This is a fairly natural development, since these functions are all add-ons to a conventional phone platform, and there is a space-saving advantage in the combination. Since Wi-Fi and Bluetooth share the same band at 2.4 GHz, they have arrangements internally that allow them to coexist or choose which service is to be used if a clash is inevitable.

In addition to the coexistence and cohabitation requirements, the antennas should fulfill the following criteria:

– **Minimum cost**. The antennas should be of low implementation cost, preferably printed and not requiring complex connectivity to the main PCB, or to require any setup and/or tuning in production;

– **Low loss**. The GPS industry is used to antennas delivering around 0–3 dB (isotropic) in an upper hemispheric direction. Obviously this will not be attainable in a mobile phone, but the gain target should be at an aggressive -4/-5 dB (isotropic);

– **Detuning**. The antennas must continue to perform to specification with any reasonable detuning environment (such as user handling, pocket, and metal surfaces);

– **Mechanical arrangement**. The antennas should be of minimum dimensions that can fit the phone mechanics. For example, long and thin may be acceptable along one side of the phone. Also placement near the GPS chip avoids lossy RF tracking;

– **Gain pattern**. Essentially omni-directional, accepting that other parts of the phone may cause localized dips in the pattern.

Considering all the elements above mentioned, the aim of this work is to provide a preliminary study able to deliver the basic guidelines for the multi-bands antenna design that best fit the compromise cost-size-performance.

In the following chapter antennas for GNSS application will be widely described with particular attention to the most suitable for the implementation in mobile phones.

Some of them are also frequently used, with some differences of course due to the different working bandwidth, also as communication antennas in mobile phones since they share the same main features (in terms of size-cost-pattern constraints) with the mobile phones GPS antennas.

In the third chapter the topic about problems related to the integration of different antennas (different bands) in the same PCB will be discussed. Also an introduction about combined (or combo) antennas will be provided.

2. GNSS Antennas

The GNSS signals are transmitted by many satellites that are on 6 different (55 degrees inclined) orbital planes located at an altitude of 20200 km above the Earth. So the satellites are not geostationary and they orbit the Earth two times per day assuring a global coverage all the time.

The current GNSS constellations are:

– The Navstar GPS constellation (USA);

– The GLONASS constellation (Russia);

– The SBAS constellations (USA, Europe, Japan, India);

– The Galileo constellation (Europe);

– The Compass (Beidou) constellation (China).

Since the GNSS satellites are scattered over the whole hemisphere, the radiation pattern of the GNSS antenna should therefore be wide in order to receive as many GNSS signals as possible.

If the antenna is oriented with its axis perpendicular to the ground, ideally a GNSS antenna should have two basic directional characteristics: a half-spherical radiation pattern and right circular polarization.

In case that the antenna is oriented in a completely random way, the antenna should be isotropic with a linear polarization so that it can receive both the RHCP and LHCP polarization even if it looses 3 dB of signal power.

In the frame of HIMALAYA project the latter is the case of interest.

Many different types of antennas are used in GNSS receivers, each of them with particular shape and performances according to the required technical specifications and particular application. Monopole antenna, dipole antenna, loop antenna, patch antenna, helical antenna, "chip" antenna and miniature high permittivity of fractal element antenna FEA are common in GNSS context ([1][2][3][4]).

2.1. Monopole Antenna

A Monopole Antenna is a $\lambda/4$ whip placed over a ground-plane. The pattern of this antenna corresponds to that of a $\lambda/2$ vertical dipole as a result of the image element posed by the ground-plane (Figure 2.1).
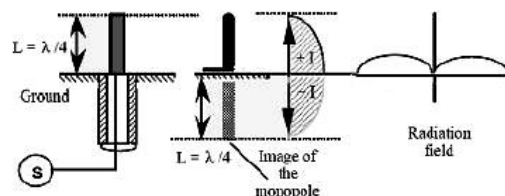
Figure 2.1: Geometry of a Monopole Antenna and its E-Plane radiation pattern.

Its input impedance is only half of the dipole (36.5 ohms). Since half of the radiating plane is cut-off by the ground-plane, the radiated power (and hence the radiation resistance) of a monopole is only half compared to the dipole with the same current; however, the directivity of a monopole antenna is doubled (3 dB larger) compared to a $\lambda/2$-dipole since the power is confined only above the ground-plane. For a finite-sized ground-plane of radius r, the pattern will tilt upward (from the ground-plane)

and this tilt would vary inversely with r/λ ratio. So the antenna needs less ground dimensions for higher frequencies. Monopole elements with perfect ideal ground-planes have a radiation pattern that has its peak on the horizon and is omni-directional in azimuth. The current on the exterior of the element feed cable is zero. For this case, the interference of the element and the image fields is totally constructive in the direction of the horizon, the feed cable is completely shielded from the element fields, and the current on the bottom surface of the ground plane is zero. For imperfect ground-planes, the direction of peak directivity are at an angle above the horizon, and the current on the exterior of the element feed cable is nonzero because the feed cable is not completely shielded from the element fields. The current on the bottom surface of the ground plane at the feed cable is also nonzero.

Monopole antenna structure generally is modified in order to make the antenna size compatible for its integration in mobile phones (see next sections).

2.1.1. Printed Multi-branch Monopole Antenna

The traditional thin monopole antenna has a simple structure and a lot of advantages, such as vertical polarization and omni-directional in a horizontal plane. Therefore it is often used in mobile phones or other mobile devices. The primary disadvantage of the antenna is its narrow bandwidth. In the past, the common way to increase the bandwidth of the thin monopole antenna is to thicken the antenna, such as conical monopole antenna and skeletal conical monopole antenna, and so on. The other means to increase the bandwidth include using load resistance or antenna folding. Compared with the thin monopole antenna, these monopole antennas appear bulky.

For the past ten more years, a broadband planar monopole antenna is developed to replace the thin monopole antenna. Due to asymmetric structure of the planar monopole antenna, a radiation pattern within a radiation frequency band changes a lot. Especially in a high frequency band, a main beam is unable to keep an omni-directional characteristic in a horizontal direction and in a vertical direction. These affect practical applications.

However, the planar antenna has the advantages of lightweight, compact size, easy manufacture, easy attachment and easy integration. Therefore applications are extensive. The planar antennas are suitable for application in wireless communication and wireless broadband system.

Generally, the methods to increase the bandwidth are using a thick dielectric substrate with a low dielectric constant, piling structure, parasitic component, or passive components such as slot, slit, integrated impedance load, chip resistance or capacitance and so on. The methods to reduce the antenna volume include using a short circuit pin, passive component (such as plate capacitance, chip capacitance or chip resistance), and slot and so on to change the current path or the antenna matching characteristics on the sheet metal.

In order to reduce the antenna volume and meet the demand of multi-band services one effective solution is to adopt a printed multi-branch monopole antenna. It is an antenna that employs a multi-branch approach, with a plurality of coupled circuits and a plurality of current paths, with each branch resonating in one band.

In [5] a printed triple-band multi-branch monopole is designed to operate in three bands for use in modern wireless systems. In Figure 2.2 there is a picture of the project layout.
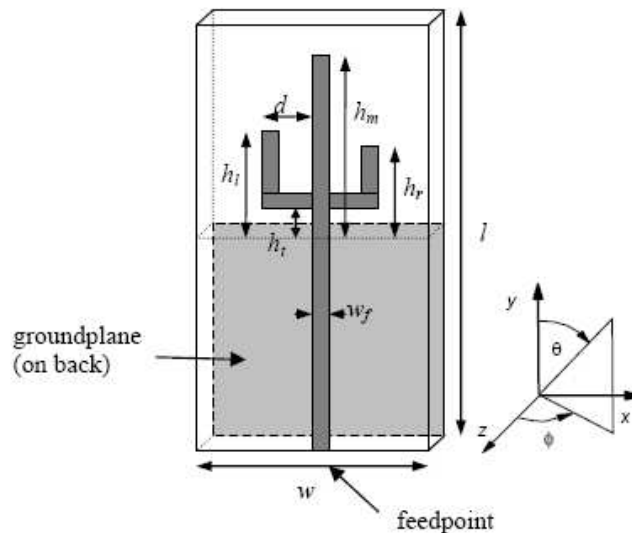
Figure 2.2: Geometry of a printed multi-branch monopole antenna.

2.1.2. Meander Monopole Antenna

This antenna mainly consists of some (generally three or four) folded meandering branches and a ground plane to meet the needs for multi-band operation and antenna size reduction requested by the mobile phone market. In fact with this kind of antennas it's possible to obtain resonant radiators shorter than 0.25 λ.

An example of a multi-band handset antenna based on this design concept and that can afford multi-band applications in the mobile systems, including GSM (880–960 MHz), GPS (centre at 1575MHz), and IMT2000 (1920–2170 MHz) bands is reported in [6]. The dimension of the proposed tri-band antenna is $41 \times 9.5 \times 6.5$ mm3 and the ground plane size is about 80×43 mm^2. A 3-D picture and a photo of the proposed antenna are present in the Figure 2.3.
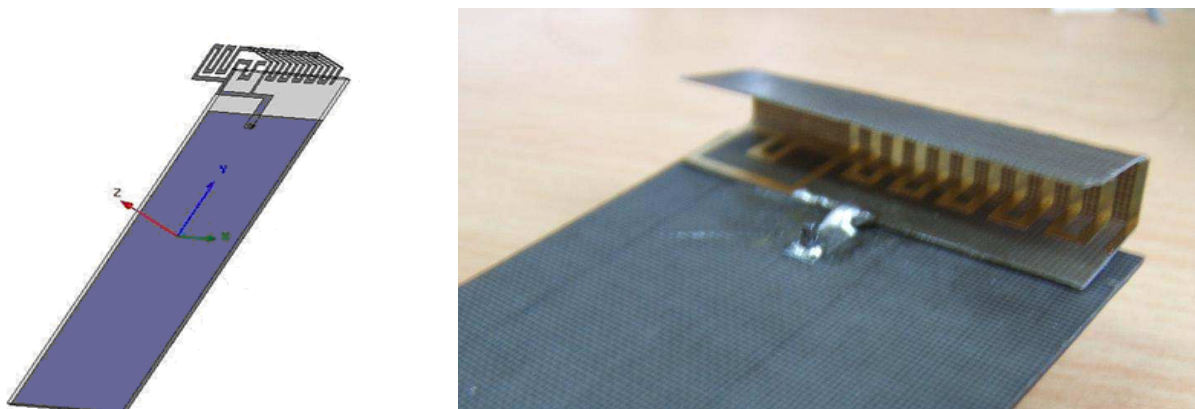
Figure 2.3: Example of a multi-band meander monopole antenna.

2.2. Dipole Antenna

A Half-wave Dipole antenna is a wire or conducting element whose length is half the transmitting wavelength and is fed at the centre. In free-space a thin dipole at resonance presents an input impedance of approximately 73 ohms. This impedance is not difficult to match to 50 ohms

transmission lines, and a number of convenient matching circuits have been designed to make the transition from various coaxial and other transmission lines. For example the mismatch of 50 ohm cable feeding a 75 ohm antenna is minimal with a resultant SWR (Standing Wave Ratio) of 1.5:1. This corresponds to roughly a 5% waste of power. A balun (BALanced to UNbalanced) allows the direct connection of a coax line to the dipole. The radiation pattern of a thin, vertical half-wave dipole in free-space has the characteristic of a doughnut shaped pattern. The E-plane antenna radiation patterns for various dipole lengths are represented in the Figure 2.4. The input impedance of a vertical dipole over a conductive ground changes compared to the impedance of a horizontal dipole placed to the same height from the ground. The distance between the dipole antenna and the conductive ground should be never lower than λ/4, and for best performance should be greater than 2λ.

To reduce the size of the dipole, several options exist:

– replacing some of the wire length with loading coils;

– bending the dipole ends back on the dipole;

– folding the dipole into a meander pattern;

– hairpin or coil loading of the center;

– capacitive loading of the dipole ends.
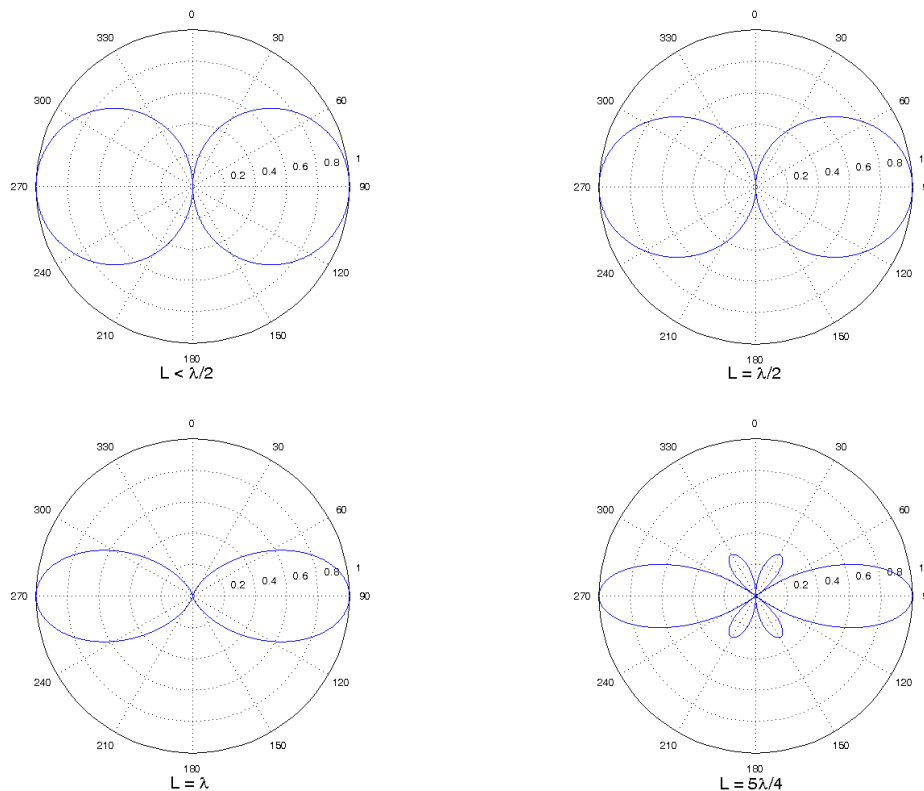
Figure 2.4: Antenna radiation patterns for various dipole lengths.

2.3. Loop Antenna

The Loop Antenna refers to a radiating element made of a coil of one or more turns. Loop antennas can be divided in three groups:

– Full-wave Loop antenna;

– Half-wave Loop antenna;

– Series-loaded, Small-loop antenna.

The **Full-wave Loop** is approximately one (λ) wavelength in circumference. Resonance is obtained when the loop is slightly longer than one (λ) wavelength. The full-wave loop can be thought of as two end-connected dipoles. Like any other loop, the shape of the full wave loop is not critical, but efficiency is determined mainly by the enclosed area. The feed impedance is somewhat higher (approximately 120 Ohms) than the half-wave loop. The main advantage of the full-wave loop is that it does not have the air gap in the loop, which is very sensitive to load and PCB capacitance spread.

The **Half-wave Loop** consists of a loop approximately λ/2 wavelength in circumference with a gap cut in the ring. It is very similar to a half-wave dipole that has been folded into a ring and most of the information about the dipole applies to the half-wave loop. Since the ends are very close together, there exists some capacitive loading, and resonance is obtained at a somewhat smaller circumference than expected. The feed-point impedance is also somewhat lower than the usual dipole, but all the usual feeding techniques can be applied to the half-wave loop. The half-wave loop is popular at lower frequencies but at higher frequencies, the tuning capacitance across the gap becomes very small and critical.

The circumference of a **Small-Loop** antenna is smaller than λ/2. The radiation resistance of the small-loop antenna is extremely small. In addition, the resistance arising from the dissipative losses can be more than ten times the radiation resistance. The radiation resistance of a small-loop can be augmented increasing the number of turns, or inserting within its circumference a ferrite core with high permeability. Typically, a small-loop may be able to radiate only a few percent of the power that comes from the transmitter. The radiation pattern of a small-loop antenna is identical with that of a small dipole. In the near-field the loop stores most of its energy in a Magnetic-H field and the short dipole stores its near-field energy in an Electric-E field, but the waves radiated by each have the same E/H; they are equally electric and magnetic.

2.4. Patch Antenna

A patch antenna consists mainly of a square (or circular) metallic conductor (patch) mounted over a ground plane. The dimensions of the patch are roughly 1/2 wavelength. The insulating space between the two planes may be air or dielectric. It should present a 50 Ohm impedance. The patch antenna is usually printed on a circuit board and can be made as part of the enclosure.

Patch antennas are flat and relatively small (Figure 2.5): the size is generally about 10 ÷ 30 mm per side and 2 ÷ 6 mm thick.

Figure 2.5: Example of a patch antenna.

Patch antennas have a good directivity, a wide cardioid radiation pattern and also their circular polarization is well controlled therefore they are well suited for GNSS applications. The gain of a typical patch antenna is about +3 ÷ +7 dBi.

In Figure 2.6 there are some examples of different beam patterns.

Ground Plane = 35mm^2
Ground Plane thickness is minimal

Ground Plane = 55mm^2
Ground Plane thickness is minimal

Ground Plane = 75mm^2
Ground Plane thickness is minimal

Ground Plane = 35mm^2
Ground Plane thickness is 6 mm
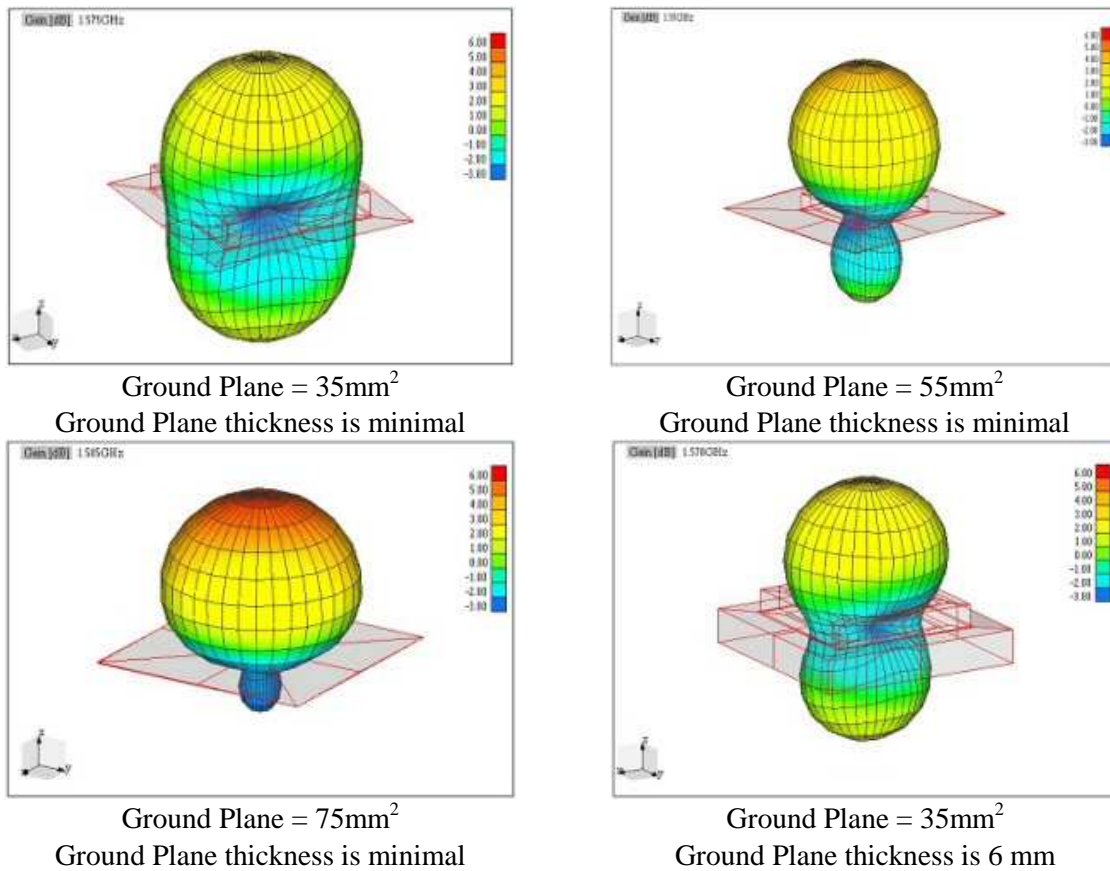
Figure 2.6: Example of radiation patterns of patch antennas.

Patch antennas are resonant and therefore their bandwidth is narrow. Consequently care must be taken to tune the size of the patch carefully. It is sensitive to the thickness and dielectric constant of the PCB and small variations will mistune the patch completely. It is also sensitive to coatings, but not extremely sensitive to hand effects. The price of this antenna is about 1÷3 $ (10 pieces) to 0.20÷0.30 $ (10k pieces) depending on the quality. Patch antennas are most used in economic applications with controlled position, like car navigation systems.

The antenna in the Figure 2.7 (Taoglas AP-10A-01) is an example of a very small, high performance and ultra low power consumption GPS active patch antenna.
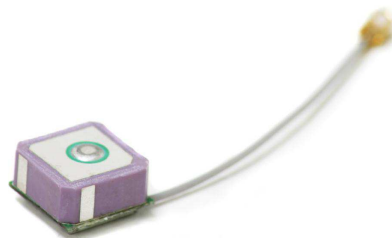
Figure 2.7: Taoglas AP-10A-01 active patch antenna.

Its main features are listed in Table 2.1:

Frequency	1575.42 ± 1.023MHz
Gain	Typ -3dBic @ Zenith
Impedance	50Ω
Polarization	RHCP
Axial Ratio	Max 4.0dB @ Zenith
Dimensions	10mm x 10mm x 4mm

Table 2.1: Main features of the Taoglas active patch antenna.

Frequently patch antennas are designed to work in two different bandwidths at the same time: e.g. in GPS L1 and L2 bands (1.227GHz and 1.575GHz). This dual-band operation is generally obtained by "stacking" two patch antennas one on top of the other, with each antenna tuned to a different frequency band. The lower frequency antenna with the wider dimensions is generally at the bottom; the smaller size, higher frequency antenna is at located at the top. The lower frequency patch acts as a small ground plane for the upper patch. Two different construction methods are shown in Figure 2.8. Typically the patch size is 50×50 mm^2.
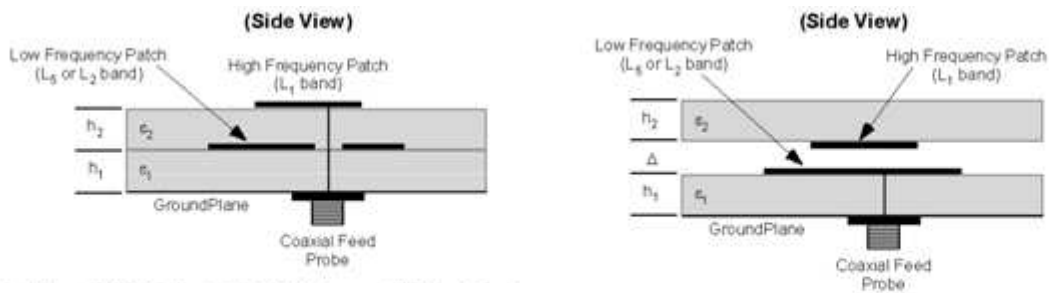
Figure 2.8: Dual-band Stack patch antennas.

However a disadvantage in both of these conventional designs is that the antennas for the two bands do not share a common dielectric substrate; the substrate for the top antenna also acts as a superstrate for the bottom antenna affecting its performance differently; this makes it difficult to optimize the design for obtaining optimum gain profile and bandwidth at both bands. The top patch also partially shields the bottom patch which can degrade its performance. When used in miniaturized adaptive antenna arrays, stacked patch antennas also suffer from increased mutual coupling from surface waves generated in the dielectric substrate that can affect gain and pattern symmetry.

These problems can be solved designing two concentric patch antennas in a co-planar geometry Figure 2.9. The inner circular patch antenna is designed to work in the GPS L1 band. Around this central patch antenna there is a thin annular ring patch antenna that is parasitically coupled to the former one; the diameter and width of the outer annular ring is tuned so that when coupled to the central patch, it resonates either in the L5 band for avionics applications or in the L2 band for military applications [7].
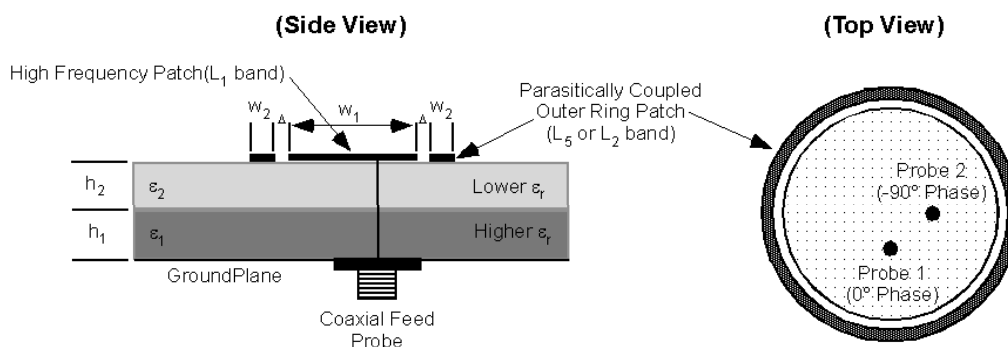
Figure 2.9: Dual-band co-planar patch antenna design.

An example of the final realization of this kind of dual-band patch antenna is represented in Figure 2.10.

Figure 2.10: Top and Side Views of Dual-Band Co-Planar Patch Antenna.

2.5. Helical Antenna

A conducting wire wound in the form of a screw thread can form a Helix antenna (Figure 2.11). Usually the Helix uses a ground plane with different forms. The diameter of the ground plane should be greater than $3\lambda/4$. In general the Helix is connected to the centre conductor of a coaxial transmission line and the outer conductor of the line is attached to the ground plane. The parameters, which characterize a Helix antenna, are:

– N = the number of turns,

– D = the diameter of the Helix,

– S = the spacing between each turn,

– L = total Length of the antenna,

– α = the Pitch angle which is the angle formed by the line tangent to the helix wire and a plane perpendicular to the helix axis.

When $\alpha = 0°$, then the winding is flattened and the helix reduces to a loop antenna of N turns.

When $\alpha = 90°$, then the helix reduces to a linear wire.

When $0° < \alpha < 90°$, then a true helix is formed.

The input impedance is critically dependent upon pitch angle and the size of the conducting wire, especially near the feed point. The main modes of operation of the Helix antenna are Normal mode (broadside) and the Axial mode (endfire).

A helical antenna radiates when the circumference of the helix is of the order of one wavelength.

Helix antennas are similar to patch antennas for some characteristics like the radiation pattern; they have a high gain, a good directivity and a relatively open cardioid radiation pattern. The smaller the antenna the wider is the radiation pattern.

The right circular polarization is normally obtained with a double helix that captures signals shifted by 90°.

The application range of these antennas goes to most of the relatively small GPS handhelds with a more or less controlled position to devices for monitoring and surveying, professional and hi-end applications. There are several double helix antenna types; geodetic antennas (typical usage), gain around 2 to 8 dBi, the more the gain, the smaller the lobe. If the antenna position is known the lobe's thickness can be reduced in order to mitigate satellites that are in horizontal position.

The cost range of Helix antennas is very broad; the average price of a helix antenna is about 1-3 $ (10X) meanwhile the average price of a double helix antenna is about 500 to 2000 $ (1X).
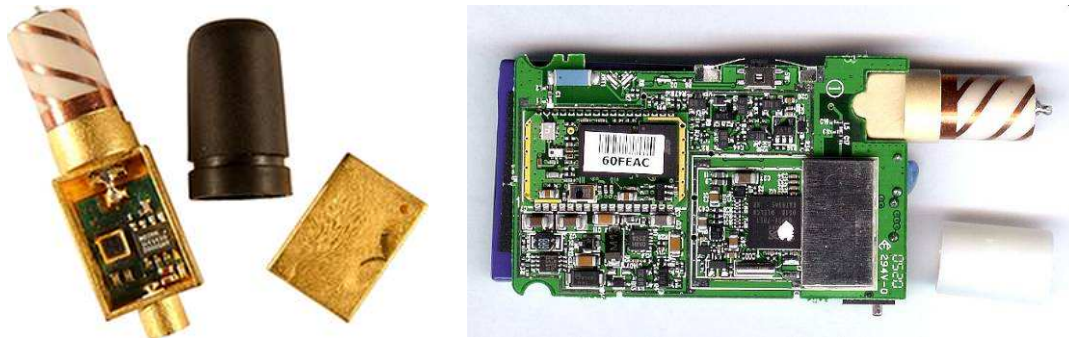
Figure 2.11: Example of helical antennas.

2.6. "Chip" Antenna

"Chip" antennas consist of a ceramic substrate with the radiating element sputtered on it. Sometimes the antenna is just a stamped metal sheet integrated somehow in the application cabinet. This kind of antenna derives from λ/4 monopole and its classical form is therefore a loaded monopole or an inverted F antenna. The construction also implies a large bandwidth.

"Chip" antennas are small in size, typically 10÷15 mm (length) by 2÷3 mm (width) by 1÷2 mm (height), making them the smallest design available (Figure 2.12). The radiation pattern of a chip antenna is not regularly shaped; its polarization is a not very well controlled linear-mixed polarization. This surface mount device is the most similar to the isotropic antenna, therefore most suited for an object used in a random position. Due to the roughly omni-directional directivity pattern the chip antenna already loses about 3dB with respect to a standard (cardioid) GNSS antenna. Moreover its small dimensions and the materials RF losses imply further losses. The sensitivity of a chip antenna is usually around -5 to -8 dBi. The cost of this antennas lies at about 0.50 \$ (10 pieces) to <0.05 \$ (>10k pieces).
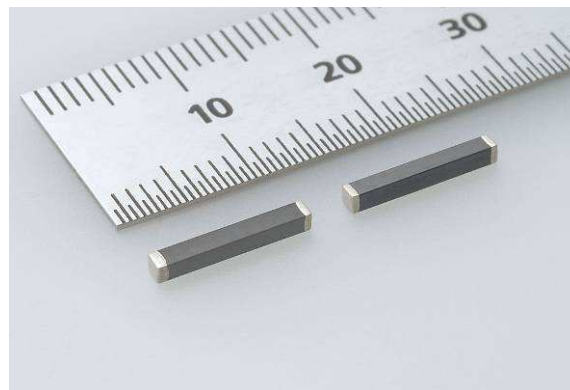
Figure 2.12: Small size chip antennas.

2.6.1. Inverted F antenna

The Inverted F Antenna (IFA) typically consists of a rectangular planar element located above a ground plane, a short circuiting plate or pin, and a feeding mechanism for the planar element. The Inverted F antenna is a variant of the monopole where the top section has been folded down so as to be parallel with the ground plane. This is done to reduce the height of the antenna, while maintaining a resonant trace length. This parallel section introduces capacitance to the input impedance of the antenna, which is compensated by implementing a short-circuit stub. The stub's end is connected to

the ground plane through a via. The antenna/ground combination will behave as an asymmetric dipole, the differences in current distribution on the two-dipole arms being responsible for some distortion of the radiation pattern. In general, the required PCB ground plane length is roughly one quarter (λ/4) of the operating wavelength. If the ground plane is much longer than λ/4, the radiation patterns will become increasingly multi-lobed. On the other hand, if the ground plane is significantly smaller than λ/4, then tuning becomes increasingly difficult and the overall performance degrades. The optimum location of the IFA in order to achieve an omni-directional far-field pattern and 50Ω impedance matching was found to be close to the edge of the Printed Circuit Board. The radiation pattern of the Inverted F Antenna is generally omni-directional with gain values that ensure adequate performance for typical indoor environments taking into account the standard values of the output power and receiver sensitivity of short range radio devices. The polarization of the antenna is rather elliptical than linear since the axial ratio rarely reaches 20 dB. Thus, the antenna has the ability to receive both vertically and horizontally polarized electromagnetic waves, which can be proven beneficial in indoor environments where depolarization is a dominant phenomenon and the choice of the best polarization difficult. The IFA bandwidth increases with its thickness. The input impedance of IFA can be arranged to have an appropriate value to match the load impedance without using any additional circuits.

Planar Inverted F Antenna (PIFA) can be considered as a kind of linear Inverted F antenna (IFA) with the wire radiator element replaced by a plate to expand the bandwidth.

– One advantage of PIFA is that it can be hidden into the housing of the mobile when comparable to whip/rod/helix antennas.

– Second advantage of PIFA is having reduced backward radiation toward the user's head, minimizing the electromagnetic wave power absorption (SAR) and enhance antenna performance.

– Third advantage is that PIFA exhibits moderate to high gain in both vertical and horizontal states of polarization. This feature is very useful in certain wireless communications where the antenna orientation is not fixed and the reflections are present from the different corners of the environment. In those cases, the important parameter to be considered is the total field that is the vector sum of horizontal and vertical states of polarization.

Narrow bandwidth characteristic of PIFA is one of the limitations for its commercial application for wireless mobile. The shorting post near the feed probe point of usual PIFA types is good method for reducing the antenna size, but this results into the narrow impedance bandwidth. Nevertheless there are several techniques to increase the bandwidth for PIFA.

– Bandwidth is affected very much by the size of the ground plane. By varying the size of the ground plane, the bandwidth of a PIFA can be adjusted. For example, reducing the ground plane can effectively broadened the bandwidth of the antenna system. To reduce the quality factor of the structure (and to increase the bandwidth), can be inserted several slits at the ground plane edges.

– Use of thick air substrate to lower the Q and increase the bandwidth.

– Using parasitic resonators with resonant lengths close to main resonant frequency.

– Adjusting the location and the spacing between two shorting posts.

– Excitation of multiple modes designed to be close together or far apart depending on requirements.

– Using stacked elements it will increase the Bandwidth.

One method of reducing PIFA size is simply by shortening the antenna. However, this approach affects the impedance at the antenna terminals such that the radiation resistance becomes reactive as well. This can be compensated with capacitive top loading. In practice, the missing antenna height is replaced with an equivalent circuit, which improves the impedance match and the efficiency. The capacitive loading reduces the resonance length from λ/4 to less than λ/8 at the expense of bandwidth and good matching. The capacitive load can be produced by adding a plate (parallel to the ground): this generates a parallel plate capacitor.

An example of a Dual-Band PIFA antenna manufactured by Shanghai Universe Communication Electronics Co. Ltd is presented in Figure 2.13.
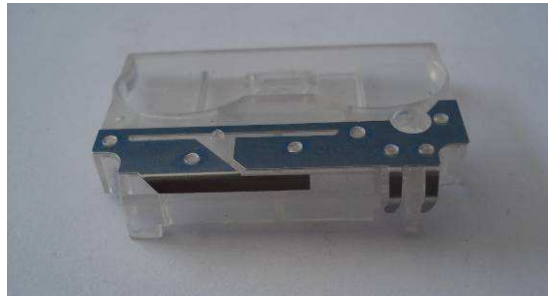
Figure 2.13: Dual-Band PIFA Antenna manufactured by Shanghai Universe Communication Electronics Co. Ltd.

Some of the main features of this antenna are listed in Table 2.2.

Name	Internal PIFA antenna
Frequency	GSM900/1800
VSWR	<= 2.5
Efficiency	>= 40%

Table 2.2: Some features of the Shanghai Universe Communication Electronics Co. Ltd Dual-band PIFA antenna.

2.6.2. Dielectric Resonator Antenna

Dielectric antennas, or antennas containing dielectrics, can have some significant advantages over conductive-only (metal) antennas.

Modern dielectrics are excellent materials to use in radio systems. They can have relative permittivities up to about 100, be low loss and have a small temperature coefficient. Generally speaking, modern low loss dielectric materials were not developed for antennas particularly, but for the dielectric resonator filter; where requirements are stringent, so good quality materials have become readily available to the antenna designer. The effective wavelength of a radio wave is shorter in a dielectric material than in free space, so one reason for using dielectrics in antennas is that they can be made smaller than conventional metal antennas. Another reason is that the antenna is generally more resistant to proximity detuning when placed close to another object (e.g., a handset antenna near your head).

The higher the dielectric constant, the better these advantages become. If the dielectric material is used in the antenna where the E-fields or RF currents are highest, then the antenna can also be more efficient than its all-metal counterpart.

Dielectrics can be used in antennas in several different ways. The earliest use is the dielectrically loaded antenna; here the metal is still the radiator but the antenna is modified by the presence of the dielectric, which gives the benefits mentioned above, but also tends to reduce the bandwidth. For many years this was the only type of dielectric antenna.

The developing of Dielectric Resonator Antennas (DRAs) [8] started in the 1980s.

DRAs are true dielectric antennas in the sense that it is the dielectric that radiates rather than any associated metal in the feed or the ground plane. An example is shown in Figure 2.14.
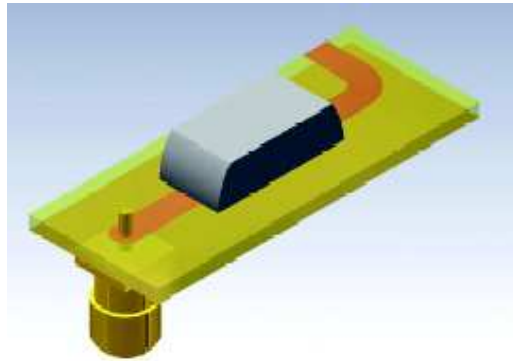
Figure 2.14: A dielectric resonator antenna designed to work at 2.4 GHz. The blue/purple material is a piece of dielectric ceramic with a relative permittivity of nearly 100.

DRAs have some excellent properties such as being small, efficient and with good resistance to proximity detuning [9]. However, they tend to have limited bandwidth, typically around 5%, whereas with modern communications systems nearer 12% to 15% is needed. The bandwidth of DRAs can be improved dramatically if the ground plane is taken away from underneath them [10] but this diminishes the advantages and is not popular with handset manufacturers who like to make use of every square millimeter of printed circuit board (PCB) available.

Another way to use dielectrics in antennas is to put them into the feed mechanism of a conventional antenna such as the (above described) planar inverted F antenna (PIFA). This has the advantage of removing some inductance and introducing capacitance into the feed network. It turns out to be much easier to design and match an antenna for wide bandwidth operation with this type of feed structure.

Dielectric resonator antennas are 3-D devices, so if the frequency of operation is halved, and the wavelength doubled, then the antenna becomes eight times bigger and heavier. This means they are usually unsuitable for use below 1 GHz. One way around this is to use the dielectric to excite a parasitic conducting antenna—this keeps many of the advantages of dielectrics, but allows a low frequency resonance to be introduced into the system without a big increase in size. Some recent multi-band handset antennas have been designed in this way; an example is shown in Figure 2.15..
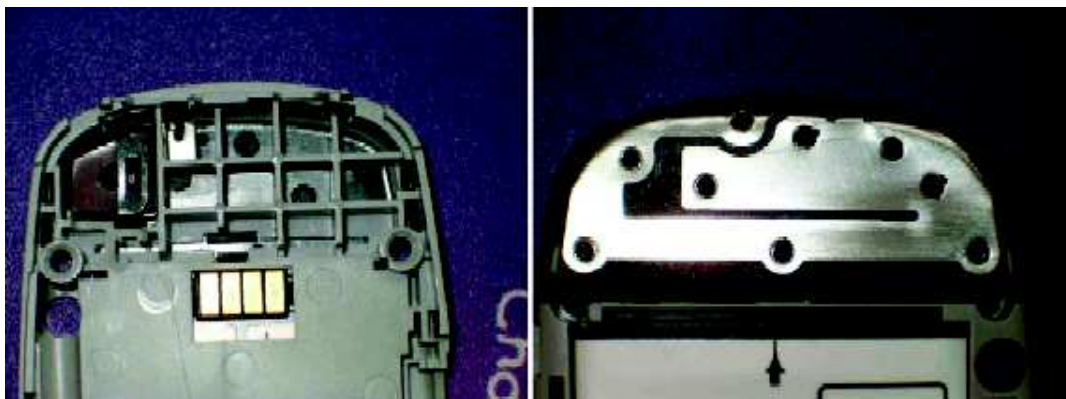
Figure 2.15: A quad-band antenna in a currently mass-produced cellular radio handset. The left hand picture shows the underneath of the antenna with the ceramic on the left hand side. The right hand picture shows the top surface and the parasitic metal component.

2.6.3. Fractal Element Antenna

A fractal antenna (Figure 2.16) is an antenna that uses a fractal design to maximize the length, or increase the perimeter of material that can receive or transmit radio wave.
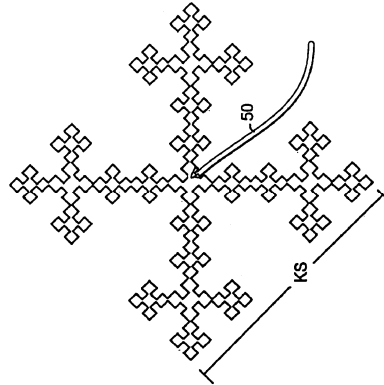
Figure 2.16: Example of Fractal Element Antenna.

Many fractal element antennas use the fractal structure as a virtual combination of capacitors and inductors. This makes the antenna so that it has many different resonances which can be chosen and adjusted by choosing the proper fractal design. Electrical resonances may not be directly related to a particular scale size of the fractal antenna structure. The physical size of the antenna is unrelated to its resonant or broadband performance. The general rule of antenna length being near target frequency wavelength does not apply itself in the same way with fractal antennas.

Fractal antennas are very compact, are multi-band or wideband, and have useful applications in cellular telephone and microwave communications.

Some studies have demonstrated that performances of patch antennas can be improved using periodic structures (Figure 2.17). Significant effort has been recently made to realize high performance antennas employing electromagnetic band-gap (EBG) structures printed on high permittivity substrates. For example a high performance GPS patch antenna can be realized with the use of the fractal high-impedance surface EBG structure. Measurements show that the GPS patch antenna offers good performance in terms of impedance and axial ratio (AR) bandwidth ([11], [12]).
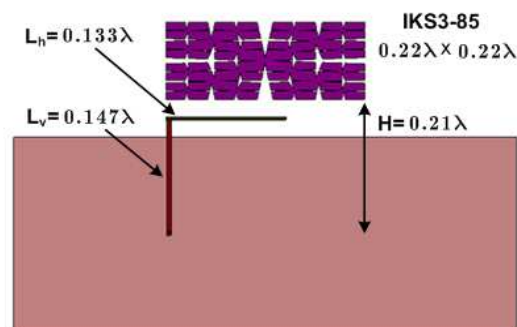
Figure 2.17: Example of a Miniature Fractal Patch Antenna.

3.   Integration Issue

The first challenge facing the RF antenna designer working on a mobile phone is the size of the whole platform. As the size of the average phone continues to fall, manufacturers are understandably reluctant to increase size again to add new features, such as GPS. Consider the wavelengths of a phone's various RF services. If the corresponding antennas were implemented as dipoles, the antennas would be bigger than the phone. Clearly the competition for antenna space is high. The designer typically wants to separate the antennas as much as possible to reduce coupling between them, both in the sense of coupling interference from one service to another (known as isolation) and in the sense of spoiling the pattern (or field) of one antenna with another ((known as interaction).

The chip business addresses the space issue through the advent of combination or combo chips, containing such peripheral services as FM (both receive and transmit), Bluetooth, GPS, and Wi-Fi. While helping with space constraints, this development brings new challenges, as these RF systems have to cohabit the same silicon and still perform individually, whatever the other RF systems are doing (transmitting/receiving GSM signal while navigating with GPS, for example). It follows that combined antennas similarly save space, but since this might involve simultaneous transmit and GPS receive functions, it is very difficult to achieve the necessary isolation, especially if the user's body can change the coupling between functions.

In many mobile phones on the market one commercially available combined antenna and two custom-made antennas are designed to fit the mechanical layout. For example the GPS antenna can be placed at the top of the phone, relegating the communications antenna to the bottom of the phone itself, where it is subject to detuning by the user's hand. Moreover the GPS antenna can be of the PIFA (planar inverted F antenna) type, working against the ground plane of the main PCB, and can be printed on a plastic molding that also implements a loudspeaker and its electrical connections.

Also the approach to the antenna system design adopted by the popular Apple iPhone 3G is very similar to the previous example. The antennas devoted to the communications services are all placed on the back side of the phone and at the bottom of the PCB. Whereas the GPS antenna is on the front side of the phone and at the top of the PCB. See Figure 3.1 for the details.
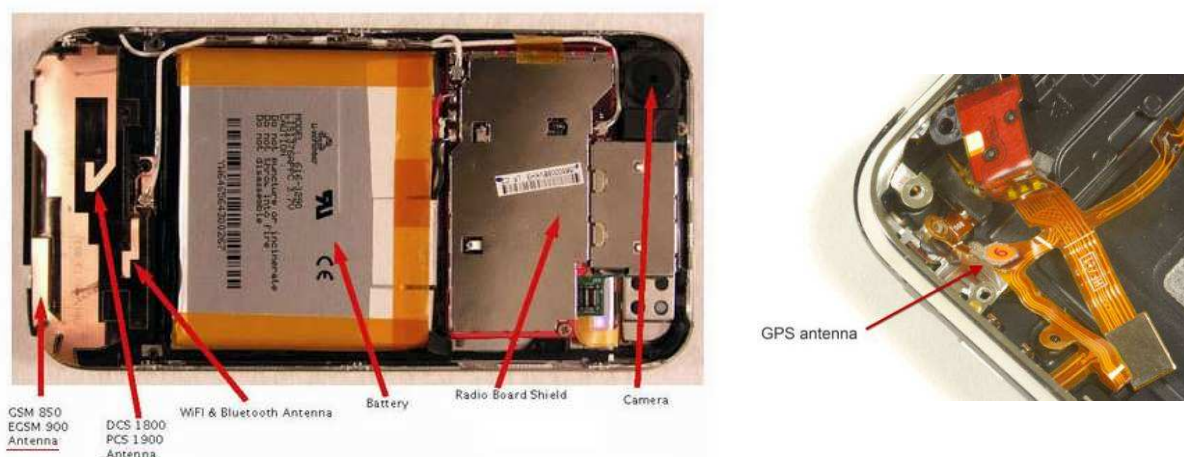
Figure 3.1: Back side view of Apple iPhone 3G and the location of the GPS antenna.

At the GPS frequencies a dipole (on FR4 PCB material) is about 8 centimetres in length, just a little shorter than the average phone platform. Changing to a monopole halves the natural length, but requires an "infinite" ground plane to work against. Ignoring this requirement, some manufacturers simply print a monopole on the main PCB, and put up with the coupling, losses, and pattern

deficiencies that arise. Designers have turned to size-reduced antennas, either by using higher dielectric materials to form them, or by using complex shape and feed derivatives.

Another idea is to use the communications antenna for GPS purpose: for example a whip-type antenna. Although the antenna is free for GPS and uses no additional space, the components to tune the whip for GPS and prevent the transmit bands reaching the GPS low noise amplifier (LNA) add both cost and size. So this is not a really too attractive solution. In this model, removing the whip and leaving the ferrule to which it connects provided a 6 dB improvement in performance (for GPS only; obviously it spoils the communications function).

A more conventional approach is to fit an off-the-shelf GPS antenna. The problem here is that any component-type antenna will have been tested with some standardized ground plane, and most are reliant on the ground plane for both tuning pattern and gain. A truly balanced design avoids this problem. Although these antennas have found favor in personal navigation devices for their superior performance, they are not usually considered for mobile phones because of cost and size considerations.

A more usual selection is the patch type, long standard in the GPS industry. The main drawback of this arrangement is the lack of a ground plane visible to the patch antenna, giving both tuning and gain/pattern problems.

The related characteristics of interference and isolation are difficult to specify and model, leading to practical measurements as the best way of accurately characterizing them. Of course, since the mechanical arrangement (including plastics, screen, battery, and PCB components) plays such a large part in determining the levels of interference and isolation, these tests can only be carried out once the phone is at the prototype stage.

Most interference we see in mobile phones gets into the GPS receiver at the antenna. Typically this is followed by an RF filter of some sort which, although it spoils the noise figure, also eliminates the out-of-band transmissions from the other RF systems on the platform. Usually there is a plethora of self-generated in-band signals that have entered the GPS receiver via the antenna. Although they can't be filtered out at all, the coupling between antenna and source can be reduced as much as possible. One effect seen in current offerings is that the GPS antenna may actually be much better at coupling to interferers than it is at extracting GPS signals from free space, thus making the problem worse.

Of course, one advantage of a poor antenna is that its coupling is likely to be less to adjacent antennas. Coupling is also seriously affected by the user holding the phone or the surface on which it is placed. Phones in a pocket seem to be more affected in this way.

Many laboratory tests have been carried out in order to measure the effective performances of antennas integrated on the phone PCB.

Typically the antenna performance is very close to the one indicated in the manufacturer data sheet when configured in its reference mechanical arrangement and not interacting with the phone environment. The antenna location on the ground plane defines its performance. This may be a problem in that the best position performance-wise is not the best for the case where the user interacts with the complete assembly. Also, the user and the plastics have a big effect.

In short, the component-type antennas currently available don't show exciting performance in a real environment, but most are competent GPS antennas when integrated according to their makers' instructions. However, this is often not possible due to mechanical and other constraints. One drawback of the monopole type of device is its need for a ground-plane-free area underneath the component, and this often conflicts with the requirements of the other antennas, which are looking to maximize the ground plane in the phone.

4. GPS Antennas on Commercial Handsets: Benchmarking Study

In this paragraph the results of the activity, fully described in the document "*20070313_GPS_Benchmarking_SAGEM.pdf*" of Sagem Wireless, are presented. The aim of reporting the activity above mentioned in this document is to benchmark the choices for the Himalaya receiver.

Some commercially available handsets were compared with regard to the GPS antenna performance. The handsets considered in this benchmarking study are:

- Sagem TiGR350 (reference handset);
- hp iPAQ;
- twig Discovery;
- hTc P3300;

An additional device, TomTom ONE, is also considered in the study. Even if it is not a handset it gives some useful information as well.

For each of them several measurements (in passive mode) have been performed: VSWR measurement in free-space and hand-held position, Antenna Efficiency measurements, Average and Peak Gain values, 2D Gain Radiation Patterns in E1, E2 and H-Planes @ 1575 MHz, 3D Gain Radiation Pattern @ 1575 MHz and Polarization.

As far as the 2D Gain Radiation Patterns are concerned, the adopted reference system together with the principal cuts is shown in Figure 4.1.
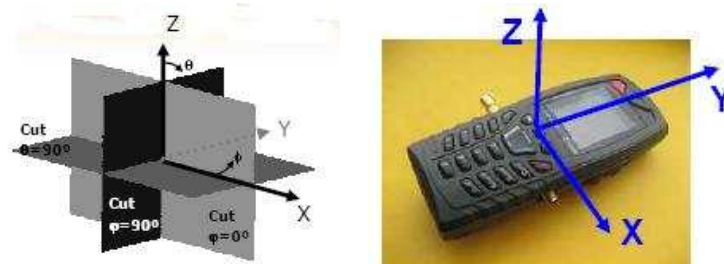
Figure 4.1: Reference system adopted to represent the 2D Gain Radiation Patterns.

The principal cuts are:

- xz-plane, Phi=0°;
- yz-plane, Phi=90°;
- xy-plane, Theta=90°.

4.1. Sagem TiGR350

The handset taken as reference is **Sagem Tigr350** (see Figure 4.2): its GPS antenna is a monopole multi-branch (see paragraph 2.1.1) whose dimensions are 37 x 10 x 0.3 mm^3, it is placed on top of the PCB and conformed to the shape of the back-cover. The material used to realize the antenna is flexfilm.

Figure 4.2: Sagem TiGR350 and its GPS antenna.

The results of the measurements are reported here following according to this order:

- VSWR and Efficiency in free space in Figure 4.3;
- Average Gain and Peak Gain in Figure 4.4;
- 2D Gain Radiation Patterns (principal cuts) @ 1575 MHz in Figure 4.5;
- 3D Gain Radiation Pattern @ 1575 MHz in Figure 4.6;
- Polarization in Figure 4.7.
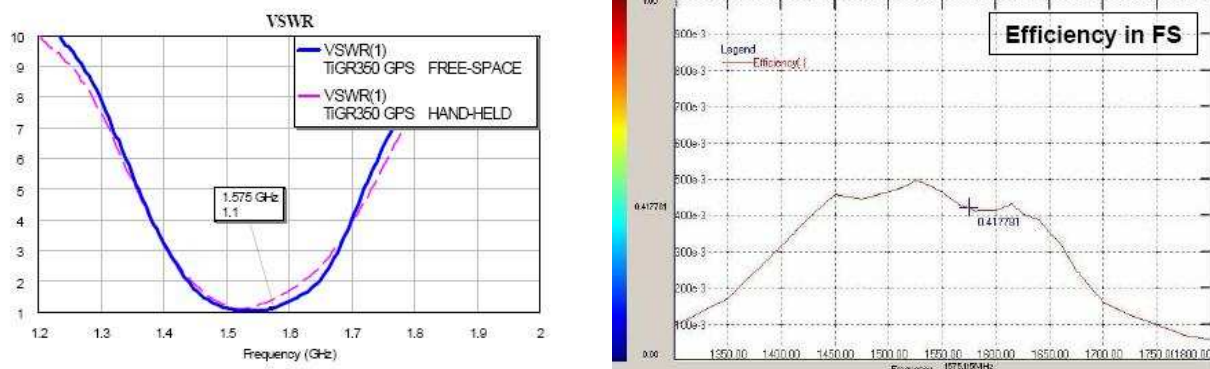
Figure 4.3: VSWR and Efficiency in free space of Sagem TiGR350.
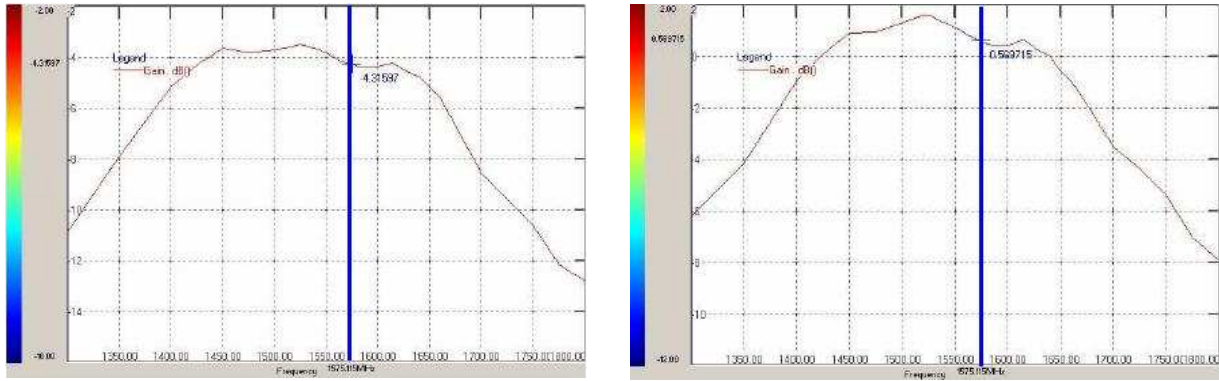
Figure 4.4: Average Gain and Peak Gain of Sagem TiGR350.

| Phi = 0° Cut | Phi = 90° Cut | Theta = 90° Cut |
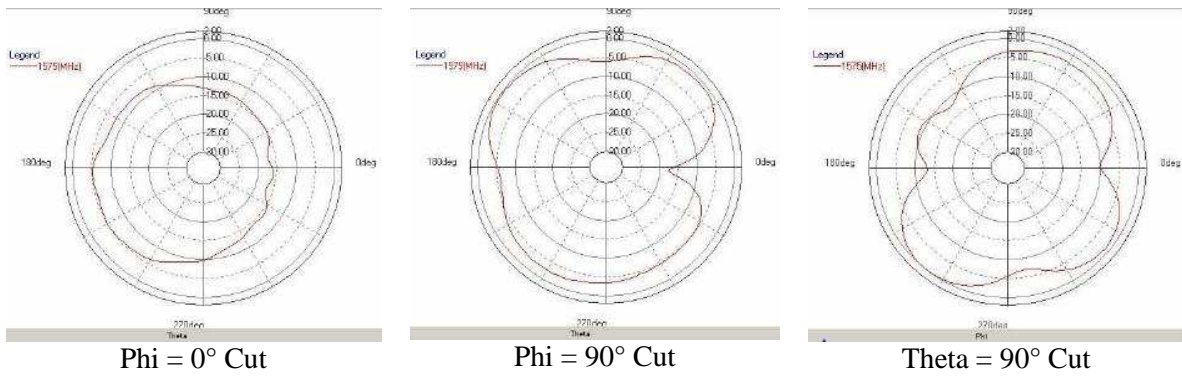
Figure 4.5: 2D Gain Radiation Patterns (principal cuts) @ 1575 MHz of Sagem TiGR350.
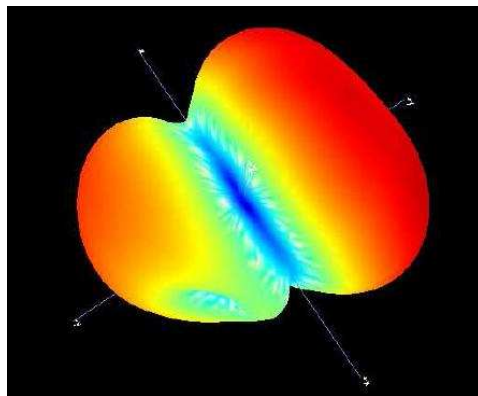
Figure 4.6: 3D Gain Radiation Pattern @ 1575 MHz of Sagem TiGR350.
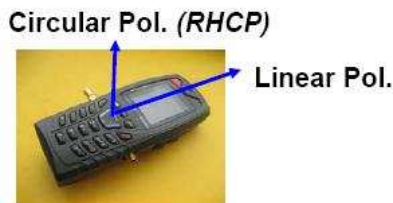
Figure 4.7: Polarization of Sagem TiGR350.

4.2. hp iPAQ

The second handset considered in the benchmarking study is **hp iPAQ**. The GPS antenna type is a meandered monopole (see paragraph 2.1.2) with dimensions 17.7 x 5.8 x 3 mm^3. The antenna is placed on top of the PCB and the material used is only metal. The pictures of the handset and its GPS antenna are reported in Figure 4.8.

Figure 4.8: hp iPAQ and its GPS antenna.

The results of the measurements are reported here following according to this order:

- VSWR and Efficiency in free space in Figure 4.9;
- Average Gain and Peak Gain in Figure 4.10;
- 2D Gain Radiation Patterns (principal cuts) @ 1575 MHz in Figure 4.11;
- 3D Gain Radiation Pattern @ 1575 MHz in Figure 4.12;
- Polarization in Figure 4.13.

Figure 4.9: VSWR and Efficiency in free space of hp iPAQ.
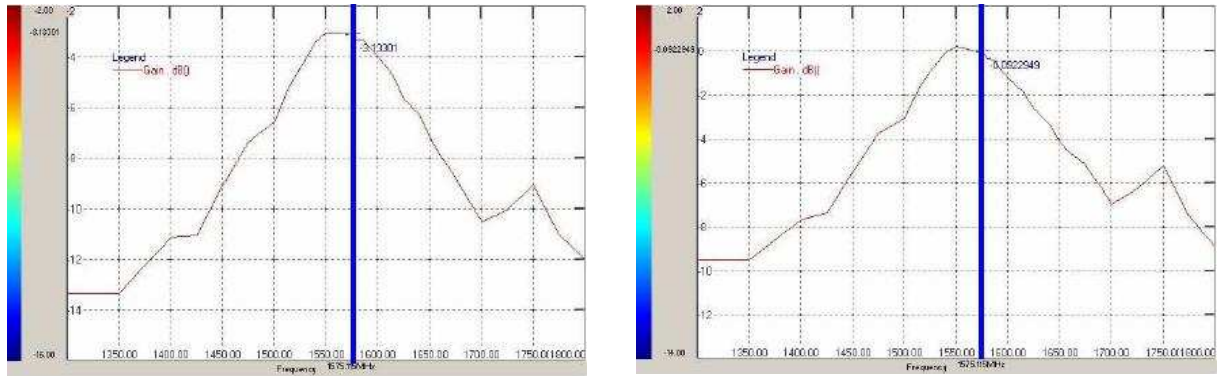
Figure 4.10: Average Gain and Peak Gain of hp iPAQ.

Phi = 0° Cut   Phi = 90° Cut   Theta = 90° Cut
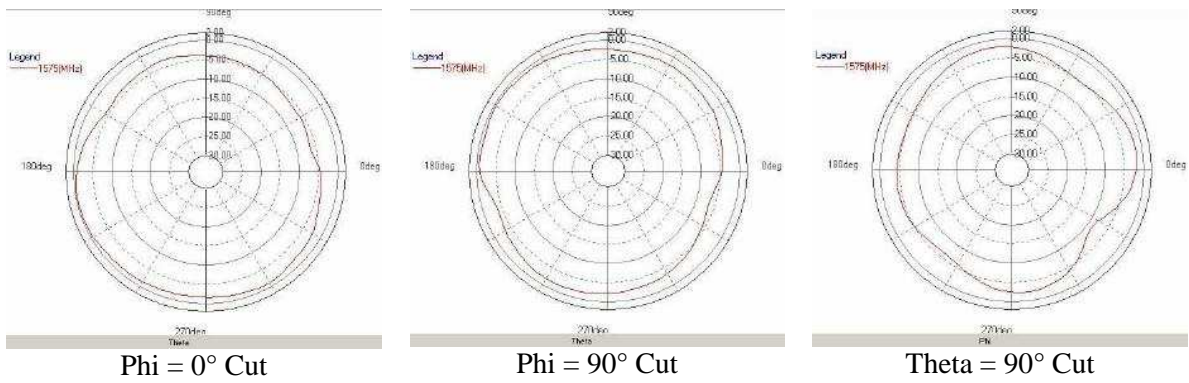
Figure 4.11: 2D Gain Radiation Patterns (principal cuts) @ 1575 MHz of hp iPAQ.
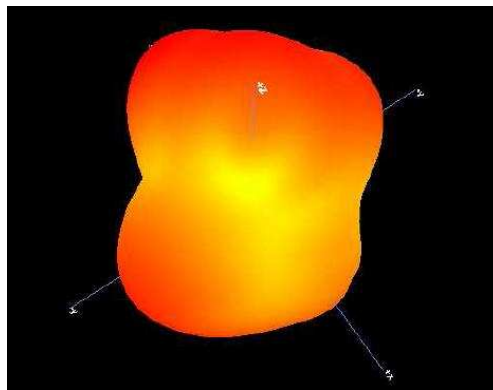
Figure 4.12: 3D Gain Radiation Pattern @ 1575 MHz of hp iPAQ.
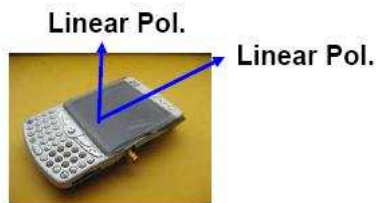
Figure 4.13: Polarization of hp iPAQ.

4.3. twig Discovery

The handset **twig Discovery** is equipped with a GPS antenna of helical (4-wires) type (see paragraph 2.5). Its dimensions are 20 x 10.7 x 10.7 mm^3 and it is on top of the PCB. The antenna is made of metal and plastics. For details about the shape of the handset and the GPS antenna see Figure 4.14.

Figure 4.14: twig Discovery and its GPS antenna.

The results of the measurements are reported here following according to this order:

- VSWR and Efficiency in free space in Figure 4.15;
- Average Gain and Peak Gain in Figure 4.16;
- 2D Gain Radiation Patterns (principal cuts) @ 1575 MHz in Figure 4.17;
- 3D Gain Radiation Pattern @ 1575 MHz in Figure 4.18;
- Polarization in Figure 4.19.
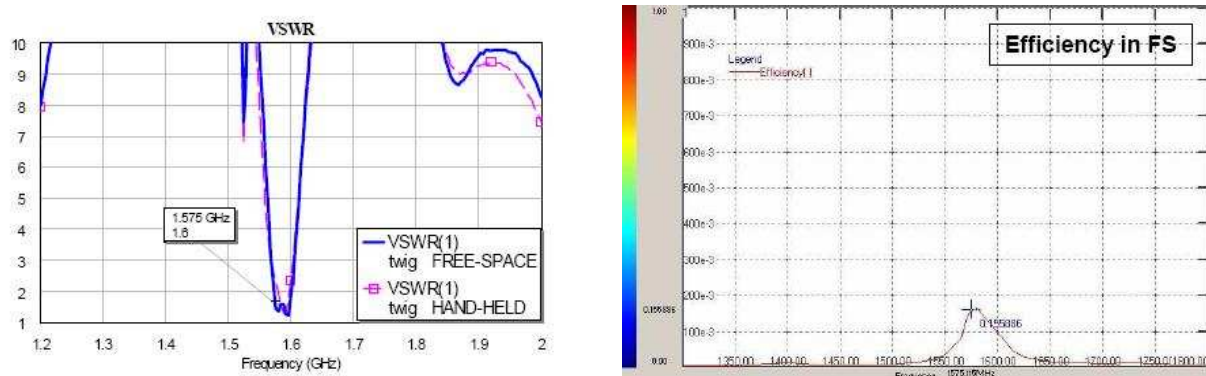

Figure 4.15: VSWR and Efficiency in free space of twig Discovery.
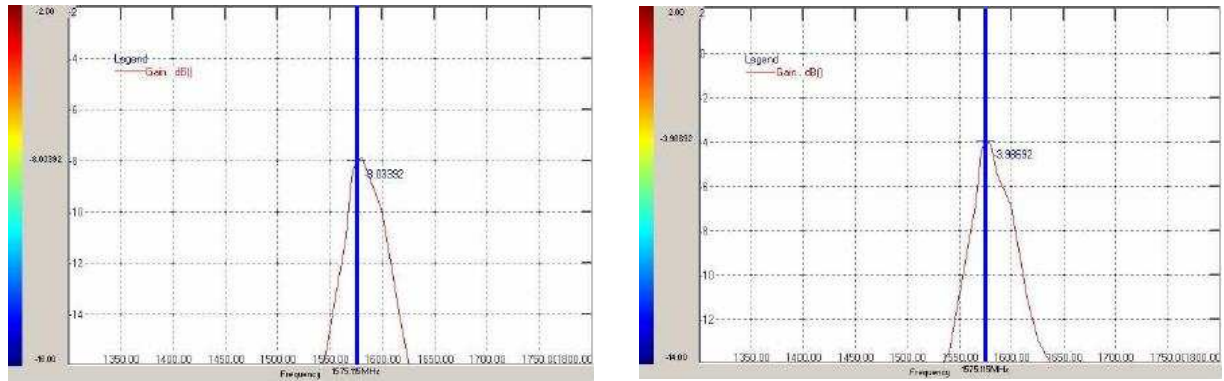
Figure 4.16: Average Gain and Peak Gain of twig Discovery.

Phi = 0° Cut   Phi = 90° Cut   Theta = 90° Cut
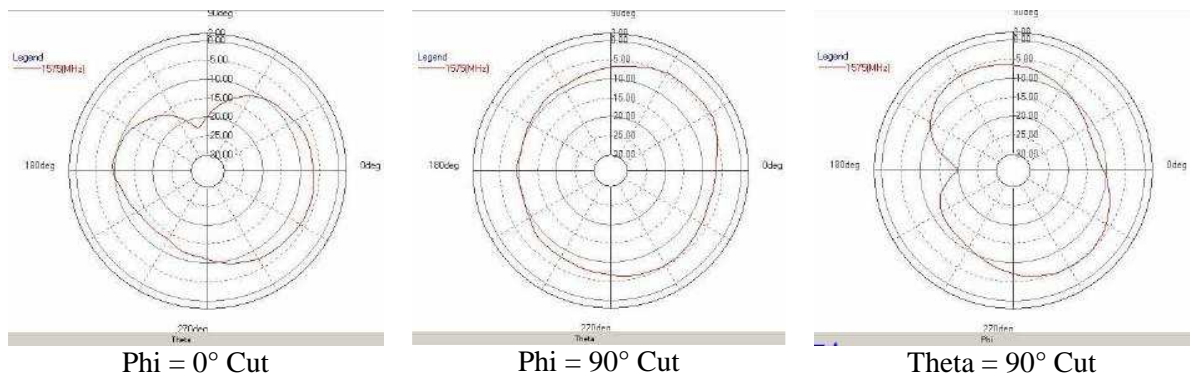
Figure 4.17: 2D Gain Radiation Patterns (principal cuts) @ 1575 MHz of twig Discovery.
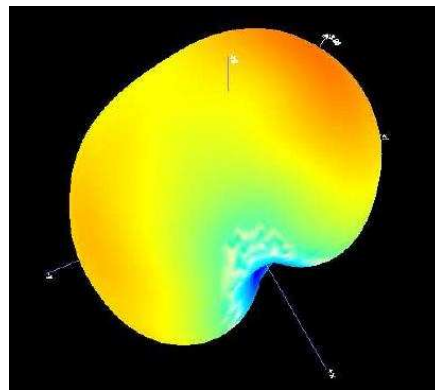
**Figure 4.18: 3D Gain Radiation Pattern @ 1575 MHz of twig Discovery.**
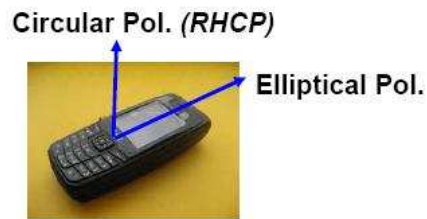
Figure 4.19: Polarization of twig Discovery.

4.4. hTc P3300

The GPS antenna integrated in the handset **hTc P3300** is a PIFA (see paragraph 2.6.1) whose dimensions are 25 x 21 x 7.2 mm^3. It is placed on top of the PCB (Figure 4.20) and it is composed of only metal.

Figure 4.20: hTc P3300 and its GPS antenna.

The results of the measurements are reported here following according to this order:

- VSWR and Efficiency in free space in Figure 4.21;
- Average Gain and Peak Gain in Figure 4.22;
- 2D Gain Radiation Patterns (principal cuts) @ 1575 MHz in Figure 4.23;
- 3D Gain Radiation Pattern @ 1575 MHz in Figure 4.24;
- Polarization in Figure 4.25.
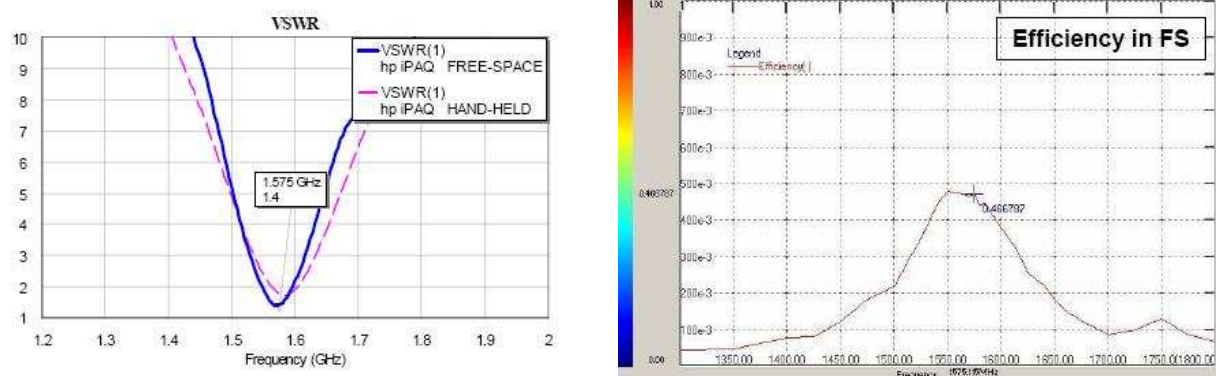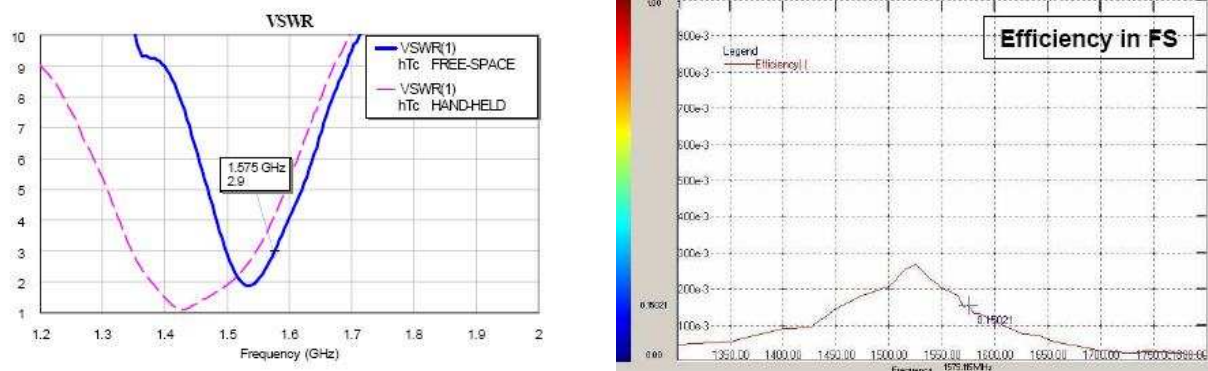

**Figure 4.21: VSWR and Efficiency in free space of hTc P3300.**
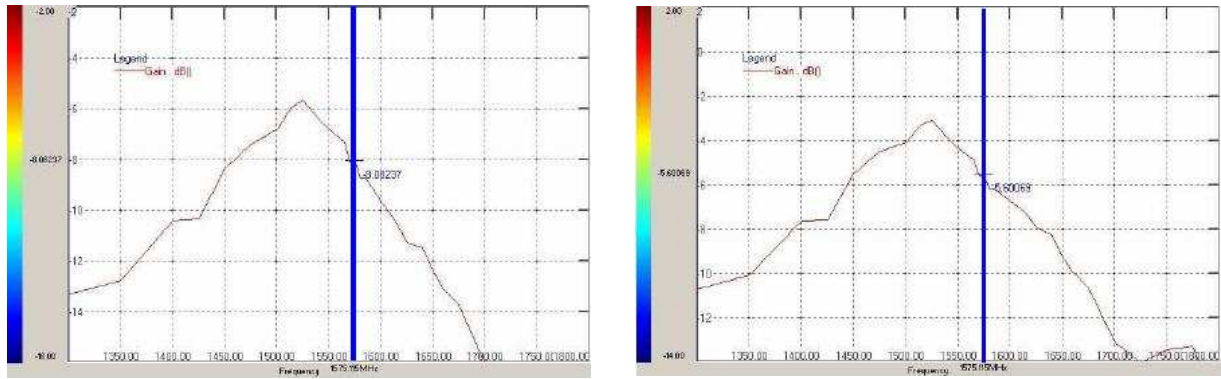
Figure 4.22: Average Gain and Peak Gain of hTc P3300.

Phi = 0° Cut   Phi = 90° Cut   Theta = 90° Cut
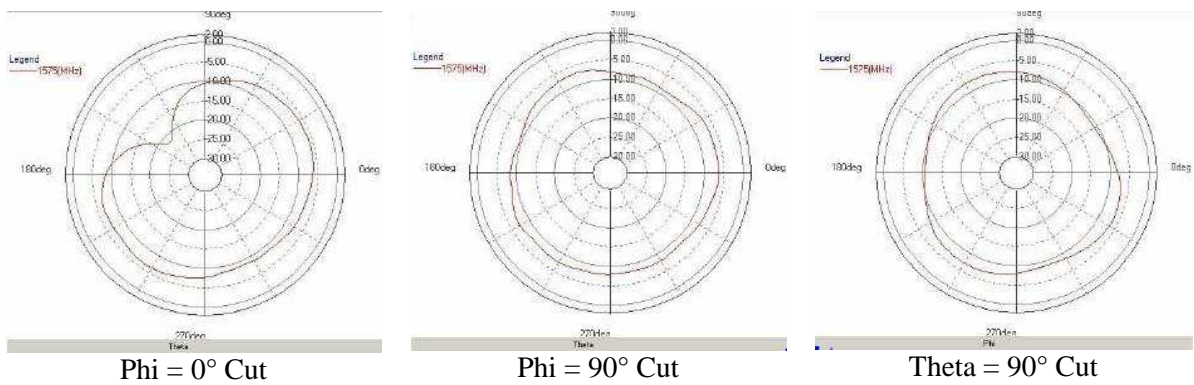
Figure 4.23: 2D Gain Radiation Patterns (principal cuts) @ 1575 MHz of hTc P3300.
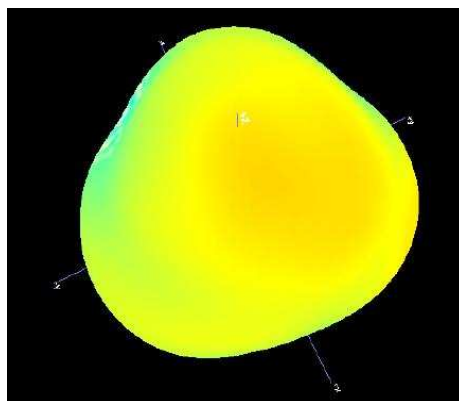
Figure 4.24: 3D Gain Radiation Pattern @ 1575 MHz of hTc P3300.
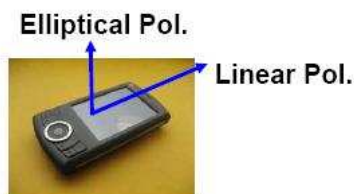
Figure 4.25: Polarization of hTc P3300.

4.5. TomTom One

The last device analysed in this benchmarking study is the **TomTom ONE**. The installed GPS antenna is an active patch (see paragraph 2.4) with dimensions 18.5 x 18.5 x 4 mm^3. The antenna is placed on top of the PCB and it is made of ceramics. The pictures showing the device and the GPS antenna are reported in Figure 4.26.

Figure 4.26: TomTom ONE and its GPS antenna.

The results of the measurements are reported here following according to this order:

- - VSWR and Efficiency in free space (measured excluding the Active Module) in Figure 4.27;
- - Average Gain and Peak Gain (measured excluding the Active Module) in Figure 4.28;
- - 2D Gain Radiation Patterns (principal cuts) @ 1575 MHz in Figure 4.29;
- - 3D Gain Radiation Pattern @ 1575 MHz in Figure 4.30;
- - Polarization in Figure 4.31.
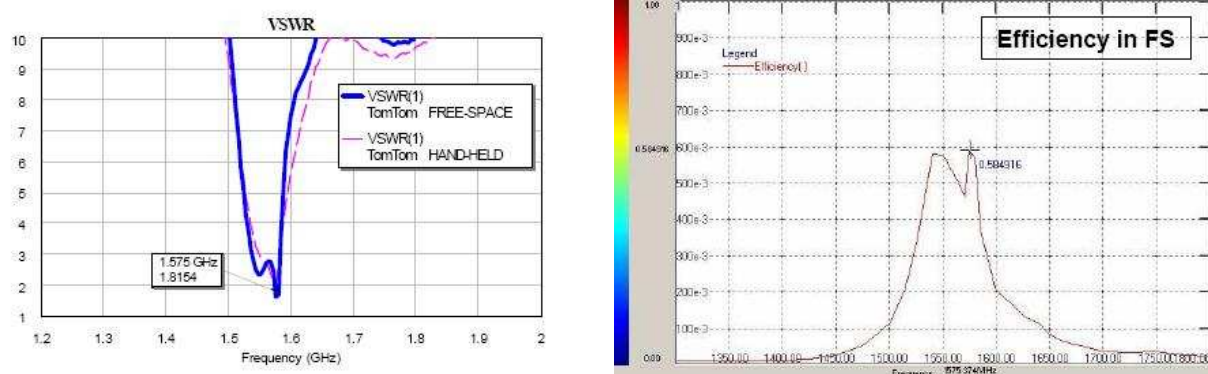
Figure 4.27: VSWR and Efficiency in free space of TomTom ONE.
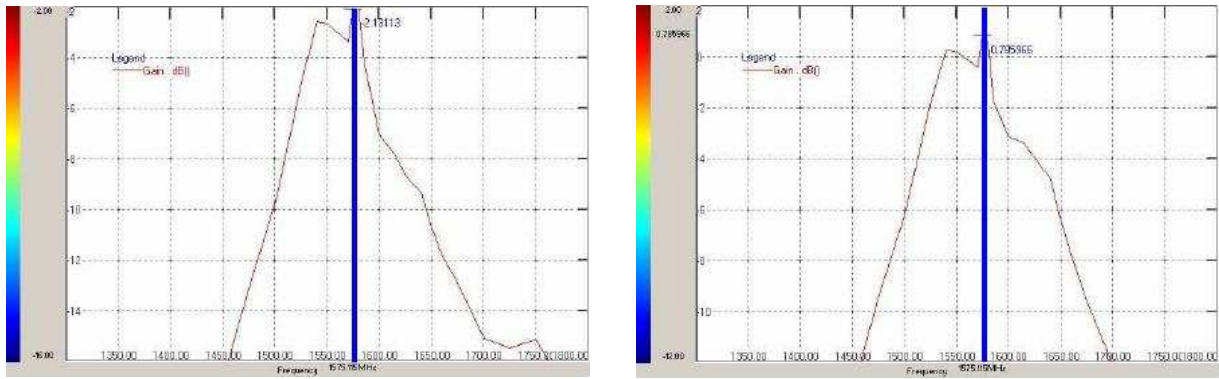
Figure 4.28: Average Gain and Peak Gain of TomTom ONE.

| Phi = 0° Cut | Phi = 90° Cut | Theta = 90° Cut |
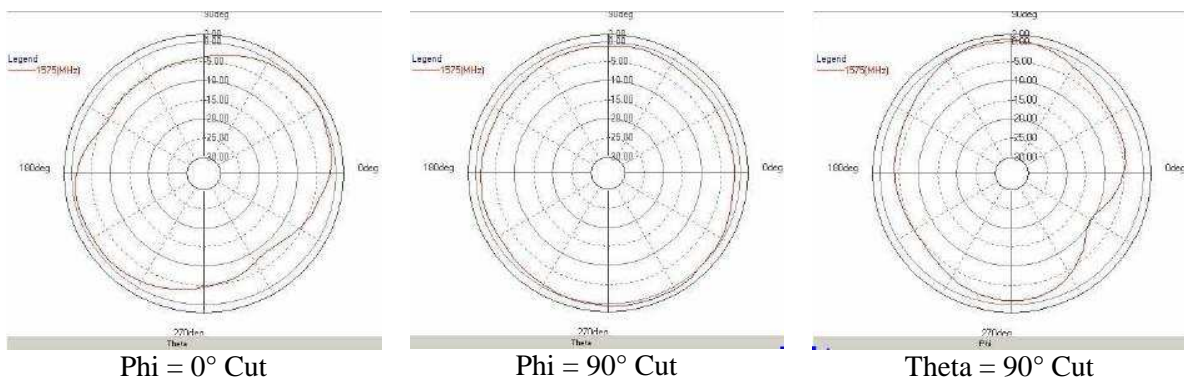
Figure 4.29: 2D Gain Radiation Patterns (principal cuts) @ 1575 MHz of TomTom ONE.
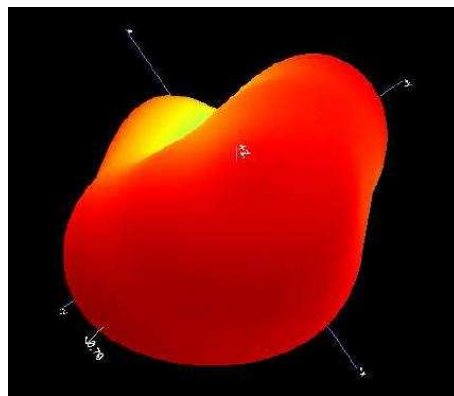
Figure 4.30: 3D Gain Radiation Pattern @ 1575 MHz of TomTom ONE.

Figure 4.31: Polarization of TomTom ONE.

4.6. Summary of Results and Conclusions

The numerical results of the measurements are summarized in Table 4.1.

|	Antenna Type	VSWR (in FS)	Efficiency (%)	Gain (dBi)		Polarization	
				Average	**Peak**	**to +Z**	**to +Y**
Sagem TiGR350	Monopole	1.1	42	-4.3	+0.6	RHCP	Linear
hp iPAQ	Monopole	1.4	47	-3.1	-0.1	Linear	Linear
twig Discovery	Helical 4 wires	1.6	15	-8.0	-3.9	RHCP	Elliptical
hTc P3300	PIFA	2.9	15	-8.1	-5.6	Elliptical	Linear
TomTom ONE	Patch (Active)	1.8	58	-2.1	+0.8	Elliptical	RHCP

Table 4.1: Summary of results of the benchmarking study.

The first comment to these results, that is quite obvious, is that the patch antenna of TomTom ONE has better GPS performance (measured in passive mode, even if the antenna is an active GPS patch) than the 4 handsets.

The 2 handsets twig Discovery and hTc P3300 have quite poor GPS performance (Gain values under usual GPS specifications).

Only hp iPAQ handset is comparable to Sagem TiGR350 in terms of Gain, but hp handset has linear polarization (in both main directions) while Sagem's has RHCP (at least in +Z direction).

So Sagem TiGR350 handset presents the best GPS performance with respect to the other considered handsets. The classification (from the highest GPS performance to the lowest) is:

- 1st – Sagem TiGR350;
- 2nd – hp iPAQ;
- 3rd – twig Discovery;
- 4th – hTc P3300.

5. Antenna Design Study for a Mobile GPS Receiver with GSM1800/UMTS and WLAN/Bluetooth Communication Interfaces

5.1. Introduction and Technical Specifications

This chapter describes a preliminary antenna design study for a mobile GPS receiver. Besides the GPS service, whose frequency band is centered at 1.575 GHz, the other considered communication standards are GSM1800 (1.710-1.880 GHz), UMTS (1.9-2.17 GHz) and WLAN/Bluetooth (2.4-2.485 GHz).

In spite of a multiband-antenna (or broadband-antenna) approach i.e. a single-port antenna working in all the required frequency bands, a combined antenna architecture has been adopted. It means that multiple antennas have been designed and properly integrated on the same printed circuit board (PCB) ([13],[14]). At first, the single antennas have been designed as a trade off between overall efficiency and spacing constraints. Afterwards, a proper positioning of the antennas on the PCB has been conceived in order to minimize the mutual coupling.

The combined architecture mainly provides a different antenna port for each receiver/transmitter. Therefore, a multiplexer is not required. Moreover, filtering requirements can be partially relaxed since significant isolation is already present between the various ports.

5.2. Antenna Design Study

5.2.1. Combined Antenna Architecture

The developed architecture is depicted in Figure 5.1. The cyan surfaces and the gray cylinders represent thin-sheet Perfect Electric Conductors (PEC) layers and PEC vias/coaxial conductors, respectively. Although all the antennas are supposed to be mounted on the package of the mobile device, no supporting dielectric structure has been considered in this preliminary work. The lower PEC layer represents the ground plane of the mobile device for which standard dimensions 100x40 mm^2 have been adopted.
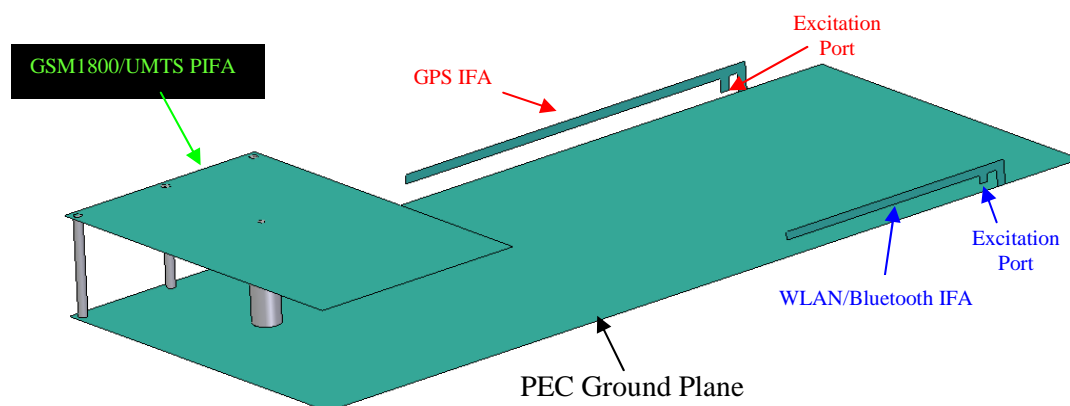
Figure 5.1: 3D model of the developed combined antenna architecture. The cyan surface is thin-sheet PEC, the gray cylinders are PEC vias and coaxial conductors.

The GPS radiator is an Inverted-F Antenna (IFA) (see paragraph 2.6.1 and [13]). It has been placed on the longest side of the ground plane due to its significant length (45.1 mm). The height of the antenna is 3.38 mm from the ground plane; the strip width is 1.1 mm.

The GSM1800/UMTS frequency bands have been covered with a single broadband Planar Inverted-F Antenna (PIFA). A basic version of the PIFA with 3 vias and a coaxial feed has been considered (see Figure 5.2). However, more advanced solutions are available in the literature ([13],[15]). The dimensions of the upper plate are 40 x 25.3 mm^2, the height is 12 mm from the ground plane and the diameter of the vias is 1 mm. The orientation of the PIFA has been selected in order to minimize the mutual coupling to the GPS antenna. For the same reason, the antenna port of the GPS radiator has been placed on the opposite side of the ground plane.

The WLAN/Bluetooth antenna consists of another smaller IFA. The antenna length is 28.9 mm, the height is 3 mm from the ground plane and the strip width is 1 mm. Even if its orientation is parallel to the one of the GPS antenna, no significant coupling occurs because of their moderately-spaced narrow bandwidths.
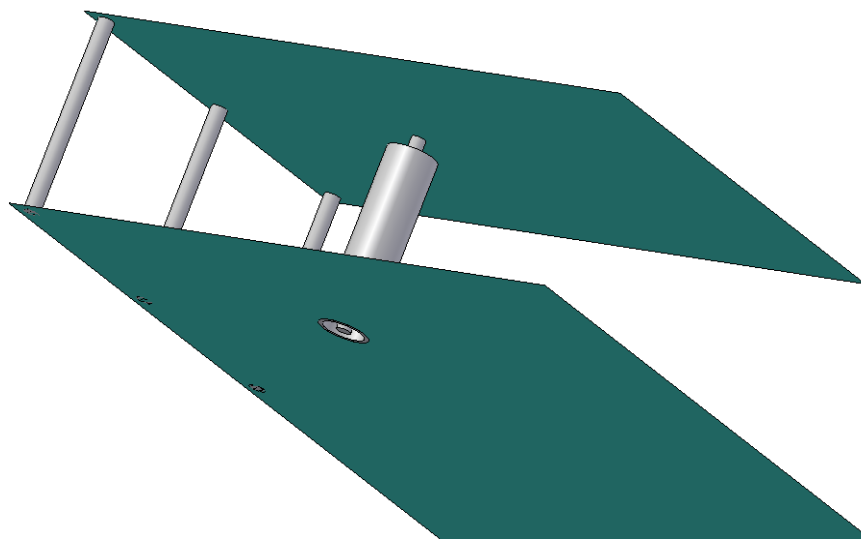
Figure 5.2: Coaxial feed excitation of the GSM1800/UMTS PIFA.

5.2.2. Results

The three antennas described in the previous section have been simulated in both the single-radiator (single antenna over ground plane) and combined-radiator configurations in order to quantify the mutual loading/coupling effect.

As far as the reflection coefficient is concerned, the obtained results are reported in Figure 5.3. Both the GPS (red curve) and WLAN/Bluetooth (blue curve) IFAs show a reflection coefficient better than -10 dB in the corresponding frequency band. A -6 dB reflection level (green curve) is instead observed for the GSM/UMTS PIFA because of the large required bandwidth. The combined-radiator response (solid curve) is very close to the single-radiator one (dashed curve) for all the antennas. Therefore, no significant degradation effect occurs owing to placement of the radiators described in the previous section.

The coupling levels between the various antennas are reported in Figure 5.4. The isolation between the two GPS and WLAN/Bluetooth IFAs is high (-30 dB, red-blue curve) because of their well-separated narrow bandwidths. More critical coupling conditions occur at lower end of the GSM1800 frequency band (1.71 GHz) where a transmitted signal at the PIFA port also reaches the GPS antenna with a -18 dB level (greed-red curve). A -20 dB coupling level is instead observed between the PIFA and the WLAN/Bluetooth IFA (green-blue curve) at the higher end of the UMTS band (2.17 GHz). The most

critical coupling condition occurs at the lower end of the WLAN/Bluetooth band (2.4 GHz) where a transmitted signal at the IFA port also reaches the PIFA port at -16 dB (green-blue curve).

The obtained coupling levels, which still require further filtering in the various receivers, can be improved by using either two different narrow-band antennas for the GSM1800 and UMTS bands or a more selective PIFA (with notches). Moreover, the solutions reported in [16], [17] can also be considered to improve isolation.
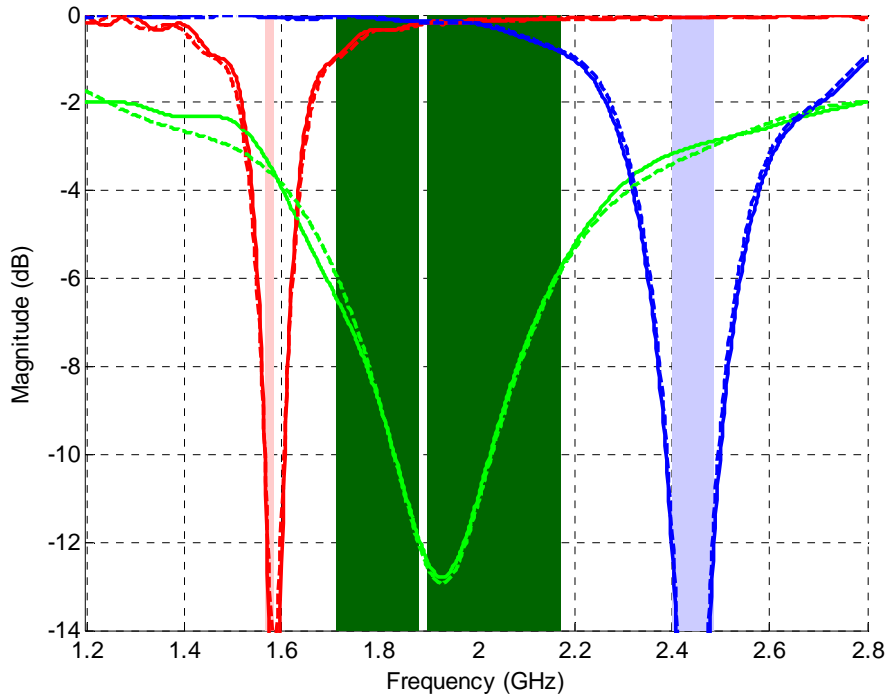
Figure 5.3: Reflection coefficient (50 Ω) of the GPS (red), GSM/UMTS (green), WLAN/Bluetooth (blue) antennas in the single-radiator (dashed) and combined-radiators (solid) configurations.
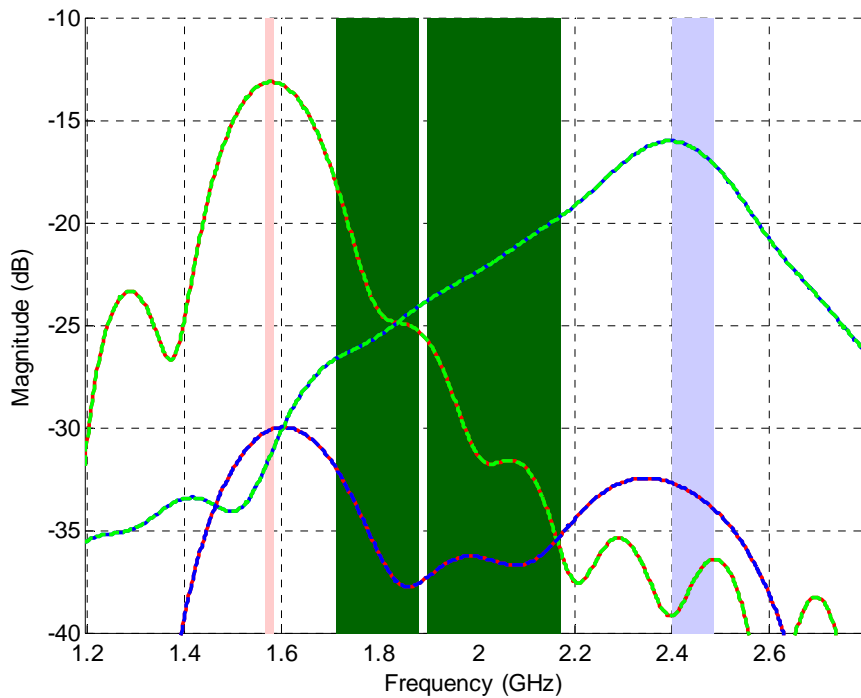
Figure 5.4: Coupling coefficients between the various antenna ports: GSM/UMTS PIFA to GPS IFA (green-red curve), GSM/UMTS PIFA to WLAN/BT IFA (green-blue) and WLAN/BT IFA to GPS IFA (blue-red curve).

Radiation patterns have also been computed for the various antennas. The adopted reference system is shown in Figure 5.5.
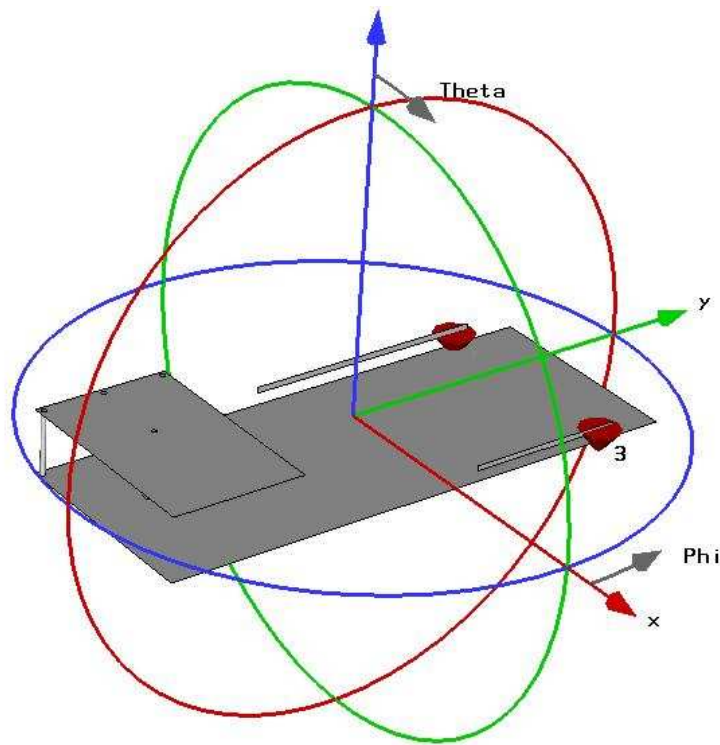
Figure 5.5: Cartesian and spherical coordinate systems.

The principal cuts such as:

- xz-plane, Phi=0°, green curve
- yz-plane, Phi=90°, red curve
- xy-plane, Theta=90°, blue curve

are reported in:

- Figure 5.6, Figure 5.7 for the GPS IFA
- Figure 5.8, Figure 5.9, Figure 5.10, Figure 5.11 for the GSM/UMTS PIFA
- Figure 5.12, Figure 5.13 for the WLAN/Bluetooth IFA.

Both the single- and combined-radiator results are reported. However, only small discrepancies can be observed for the two different operative conditions.

As expected, all the antennas have a quite omni-directional radiation pattern. Therefore, they are suitable for a mobile application.
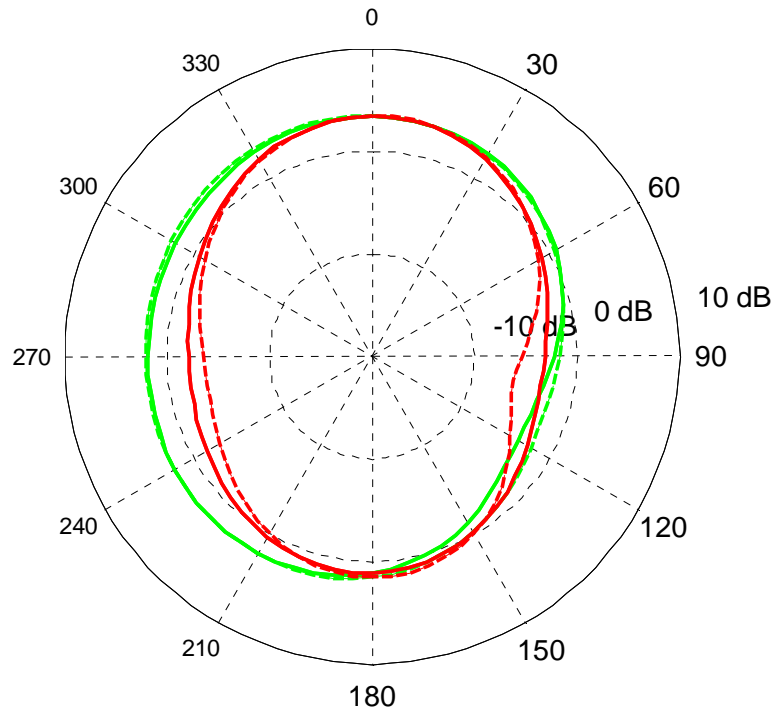
Figure 5.6: Radiation pattern of the GPS IFA @1.575 GHz in the single-antenna (dashed line) and combined-antenna (solid line) configurations. The green and red curves represent the Phi=0°and Phi=90° cuts, respectively.
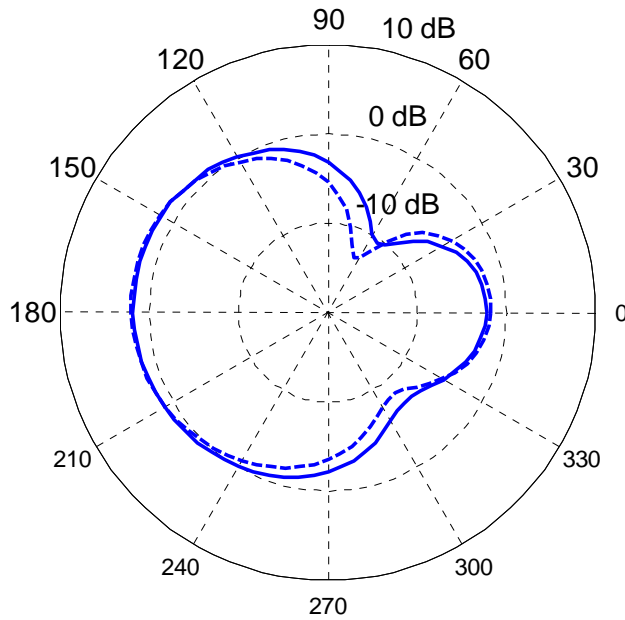
Figure 5.7: Radiation pattern (Theta=90° cut) of th e GPS IFA @1.575 GHz in the single-antenna (dashed line) and combined-antenna (solid line) configurations.
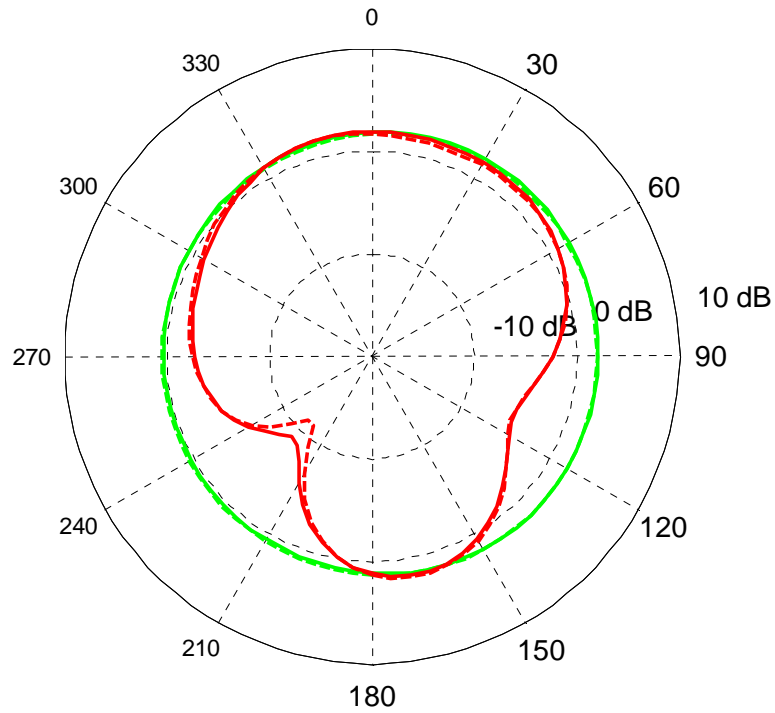
Figure 5.8: Radiation pattern of the GSM/UMTS PIFA @1.795 GHz in the single-antenna (dashed line) and combined-antenna (solid line) configurations. The green and red curves represent the Phi=0°and Phi=90° cuts, respectively.
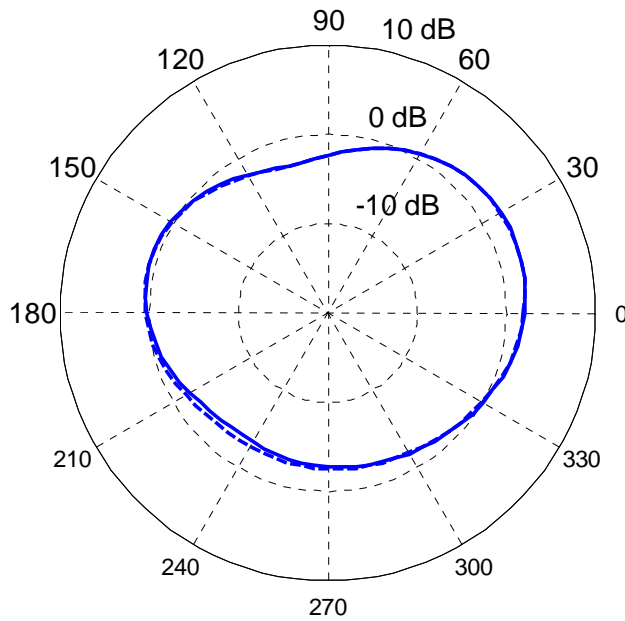
Figure 5.9: Radiation pattern (Theta=90°cut) of th e GSM/UMTS PIFA @1.795 GHz in the single-antenna (dashed line) and combined-antenna (solid line) configurations.
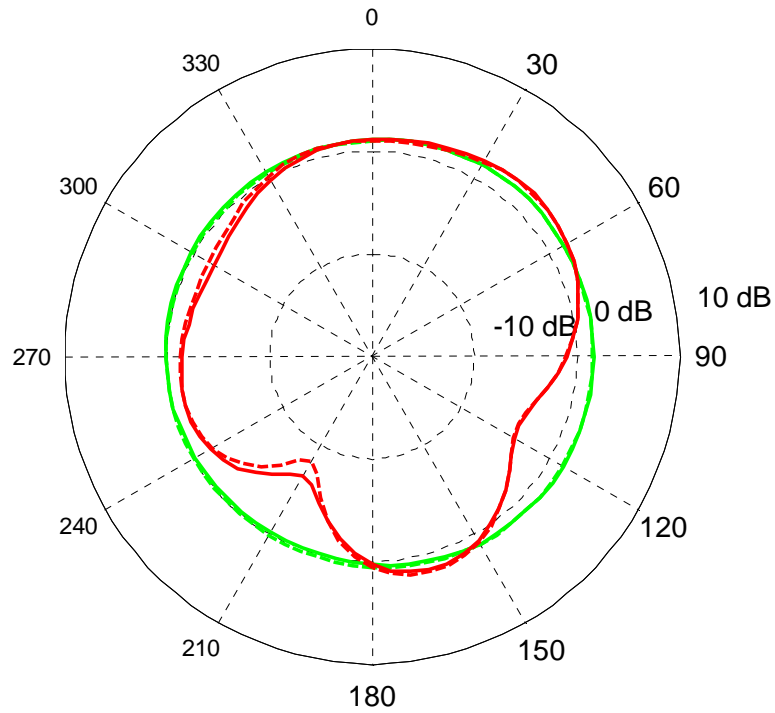
Figure 5.10: Radiation pattern of the GSM/UMTS PIFA @2.035 GHz in the single-antenna (dashed line) and combined-antenna (solid line) configurations. The green and red curves represent the Phi=0° and Phi=90° cuts, respectively.
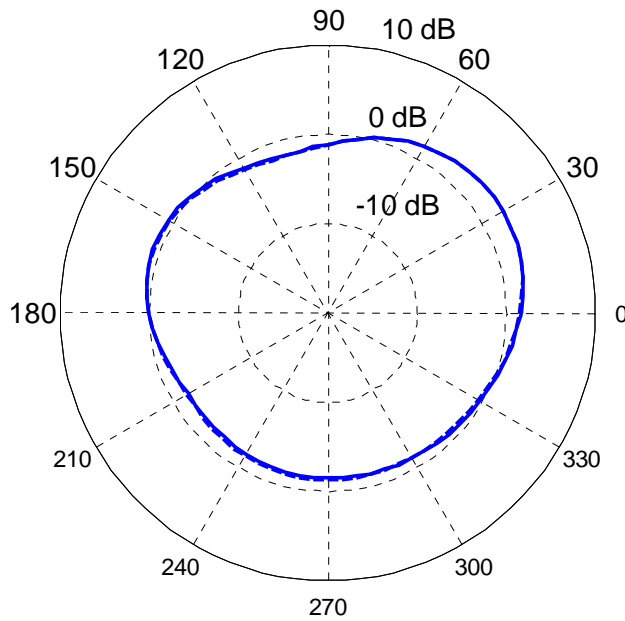
Figure 5.11: Radiation pattern (Theta=90° cut) of t he GSM/UMTS PIFA @2.035 GHz in the single-antenna (dashed line) and combined-antenna (solid line) configurations.
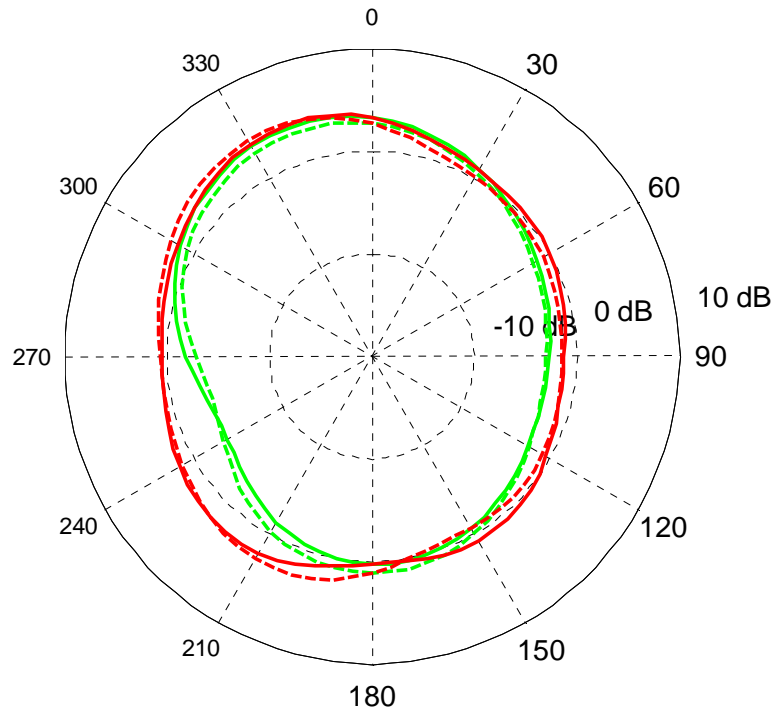
Figure 5.12: Radiation pattern of the WLAN/BT IFA @2.44 GHz in the single-antenna (dashed line) and combined-antenna (solid line) configurations. The green and red curves represent the Phi=0° and Phi=90° cuts, respectively.
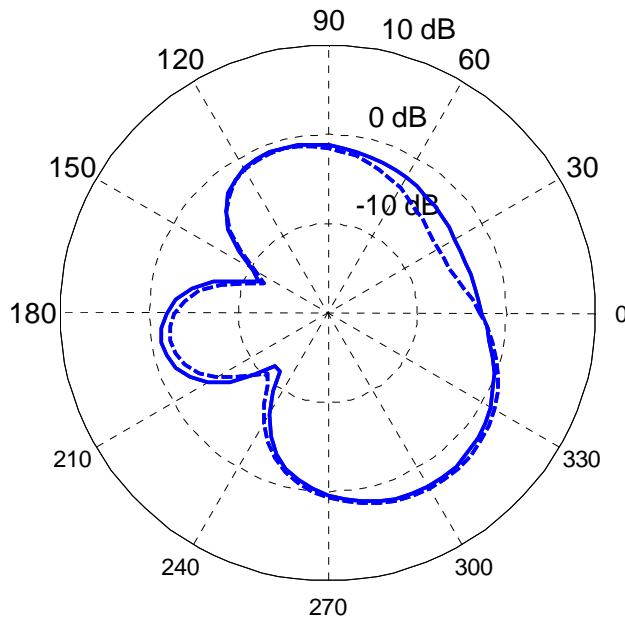
Figure 5.13: Radiation pattern (Theta=90° cut) of t he WLAN/BT IFA @2.44 GHz in the single-antenna (dashed line) and combined-antenna (solid line) configurations.

6. Beam-forming Architecture

The term *Beam-forming* generally means the combination of signals coming from an array of small non-directional antennas (Figure 6.1) so that it is synthesized a great directional antenna that receives the signal coming from a well precise direction, limiting the contribution of signals coming from other directions. The synthesized antenna can be electronically steered without any physical motion.
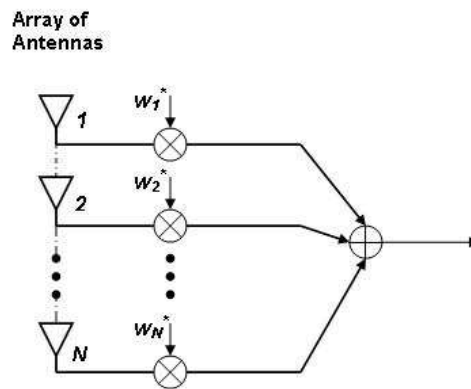
Figure 6.1: General architecture of a narrowband beam-former.

In other words beam-forming indicates the technique by which it is realized a versatile form of spatial filtering that allows separating out signals that are spectrally overlapped but that come from different spatial directions.

Antenna arrays using beam-forming techniques can reject interfering signals by pointing the radiation nulls towards the direction of arrival of the interferers (Figure 6.2).
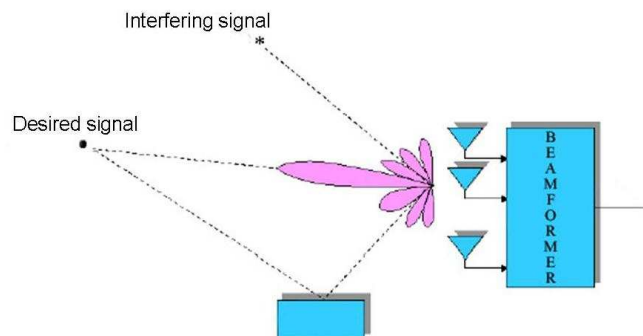
Figure 6.2: Spatial filtering realized thanks to the beam-forming technique.

Array beam-forming techniques also allow to simultaneously form a certain number of beams exploiting analogue or digital processing methods. The beams can be formed so that they offer high gain and low sidelobes, or controlled beamwidth.

Adaptive beam-forming techniques adjust on the fly the array beam-pattern in order to optimize some characteristics of the received signal. For example, in beam-scanning a single main beam of an array can be continuously steered in different directions within the field of view (beam size of the single antenna element).

6.1. Introductive notes

In order to introduce some of the most popular beam-forming algorithms, it is convenient (for simplicity reasons) to consider a generic linear array whose elements are equally spaced (with an inter-element spacing of *d*) without loss of generality.

We can also assume that the signal received by the array is a plane wave (Far-Field source), with *Direction of Arrival* (*DOA*) θ and frequency ω, and we can consider the signal received by the first element of the array as the reference with null phase.

The *beamformer response* to this kind of signal can be easily expressed in vector form:

$$r(\theta, \omega) = \boldsymbol{w}^H \boldsymbol{d}(\theta, \omega) \qquad (6\text{-}1)$$

w is the vector containing the beamformer coefficients that have to be multiplied by the time samples coming from the antennas, $(\cdot)^H$ is the Hermitian operator and $\boldsymbol{d}(\theta, \omega)$ is the *response vector of the array*, also called *steering vector* or *directional vector*.

With the hypothesis made before and supposing that the array is calibrated and the antennas of the array are ideal (omnidirectional antennas), the elements of the vector $\boldsymbol{d}(\theta, \omega)$ are:

$$\boldsymbol{d}(\theta, \omega) = \begin{bmatrix} 1 & e^{j\omega\tau_2(\theta)} & \cdots & e^{j\omega\tau_N(\theta)} \end{bmatrix}^H \qquad (6\text{-}2)$$

where $\tau_i(\theta)$, for $2 \leq i \leq N$, are the time delays due to the signal propagation (Figure 6.3).
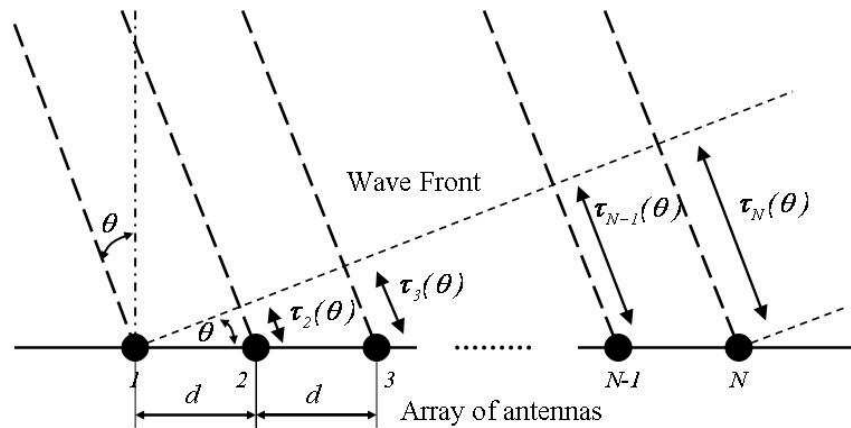
Figure 6.3: A plane wave with *DOA* θ and frequency ω is received by a linear array of *N* antennas.

The ideal steering vector (6-2) takes into account the geometry of the array.

The non ideal characteristics of the antennas and receiver electronics (not calibrated electronics, directional antennas, ...) can be included in $\boldsymbol{d}(\theta, \omega)$, multiplying it by a function $\boldsymbol{a}(\theta, \omega)$ that depends on the response of each receiver chain (antennas, LNAs, ...) for that particular *DOA* θ and frequency ω.

The time delays $\tau_i(\theta)$ can be also written in the form:

$$\tau_i = \frac{(i-1)\,d\,\sin\theta}{c} = \frac{(i-1)\,d\,\sin\theta}{\lambda\,f} \tag{6-3}$$

for $2 \le i \le N$, so the steering vector becomes:

$$d(\theta,\omega) = \left[\begin{array}{cccc} 1 & e^{j2\pi\frac{d}{\lambda}\sin\theta} & \ldots & e^{j2\pi(N-1)\frac{d}{\lambda}\sin\theta} \end{array}\right]^H \tag{6-4}$$

6.2. Data-Independent Beam-forming

In the data-independent beam-forming the coefficients are chosen so that the beam-former response is as close as possible to a desired known a priori response, regardless of the sequence of data or their statistics.

Following this approach it is possible to synthesize the beam in the classical way, i.e. maximum value of the response in only one direction and zero elsewhere. There are also more general methods for beam-forming system design that allow having arbitrary types of response.

6.2.1. Beam-steering algorithm

The **Beam-steering** or **Classical Beam-forming Algorithm** simply aims to separate a signal coming from a certain known direction θ_0 from the other received signals arriving from different directions.

Supposing the signal is narrowband (at frequency ω_0), the desired response of the beam-former is ideally equal to one for (θ_0,ω_0) whereas it is null elsewhere.

A common solution to this problem consists of taking the *steering vector* $\boldsymbol{d}(\theta_0,\omega_0)$ as the vector of the coefficients $\boldsymbol{w}$:

$$\boldsymbol{w} = \boldsymbol{d}(\theta_0,\omega_0) \tag{6-5}$$

It is demonstrated that this solution is the best choice in order to minimize the square error between the ideal and the real response.

The response is characterized by a *main lobe*, also called *beam*, and many *secondary lobes* (*sidelobes*).

Generally the narrower the beam and the lower the level of the sidelobes the better the response.

The combination of array of antennas/beam-former is also called *phased array* since the relative phases of the antenna output signals are varied before these signals are summed.

From (6-5) and (6-2) it can be noticed that the amplitude of every element of $\boldsymbol{w}$ is equal to one.

So it is possible to apply a windowing algorithm to the coefficient vector $\boldsymbol{w}$ (modifying the amplitudes of all its elements) in order to obtain the best trade-off between the main lobe and secondary lobes levels. However this causes inevitably a loss of resolution: in fact the beam becomes a bit larger.

In Figure 6.4 there is an example showing the effect of coefficient windowing that allows the control of the array beam-pattern shape. For this example it has been considered a linear array composed of 16 omni-directional antennas with an inter-element spacing of $\lambda/2$.

On the left side of the figure it is reported the beam-pattern of a classical narrowband beam-former whose beam is pointing the direction $\theta_0 = +20°$. On the right side of the figure the windowing

(Hamming algorithm) of beam-former coefficients is applied: this way the secondary lobes are kept to a lower level (-40 dB) but the beam results to be slightly wider.
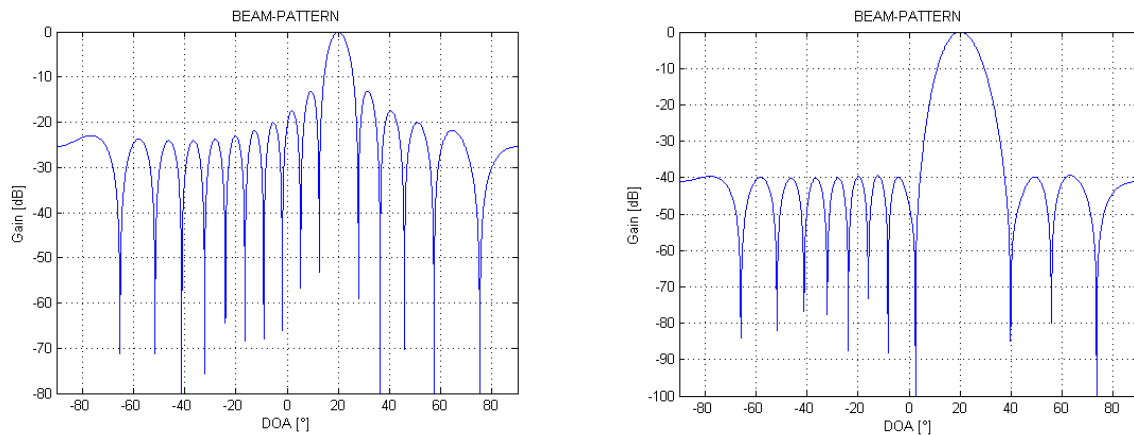
Figure 6.4: Beam-pattern of classical narrowband beam-former in the case of a linear array of 16 omni-directional antennas, with pointing direction +20° and without any windowing of the coefficients (left side). On the right side of the figure the coefficients have been windowed according to the Hamming algorithm.

6.3. Statistically Optimal Beam-forming

In the statistically optimal beam-forming the coefficients are chosen on the basis of the statistics of the data received by the array.

The target is to optimize the beam-former response so that the output has the minimum contribution due to noise and undesired signals (having *DOA* different from the one of the desired signal).

6.3.1. Multiple Sidelobe Canceller (MSC)

The **Multiple Sidelobe Canceller (MSC)** consists of a *primary channel* and one or more *auxiliary channels*, as schematically represented in Figure 6.5.
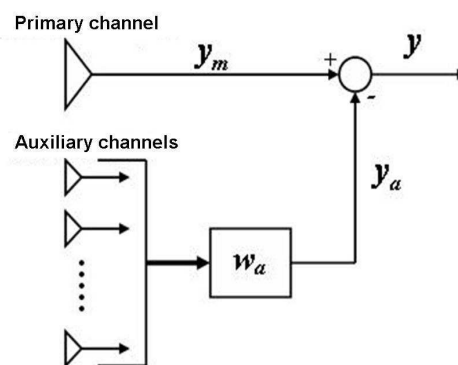
Figure 6.5: Principle scheme of the MSC beam-former.

The primary channel can be a single high gain antenna or a data-independent beam-former. It has a highly directive response in the direction of the desired signal θ_d. Besides, the interfering signals (with *DOA* θ_i) are supposed to be received by the sidelobes of the primary channel and by the auxiliary channels as well. The coefficients of the auxiliary channels $\mathbf{w_a}$ have to be chosen in order to cancel the component of the interference that is present in the primary channel. It follows that the response of the primary channel due to the interfering signals has to be equal to a linear combination of the auxiliary channels. The output response of the system is similar to the one represented in Figure 6.6.

Primary channel response

Auxiliary channels response

Output response
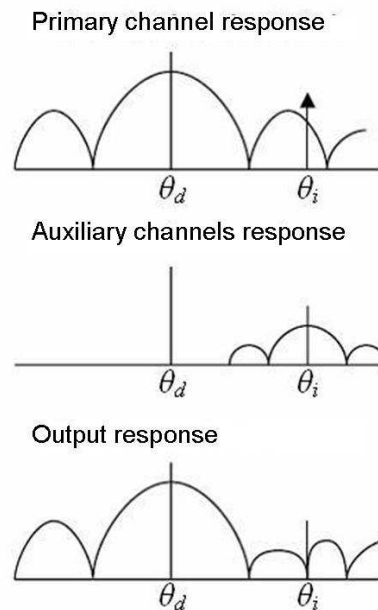
Figure 6.6: Cancellation of an interfering signal with *DOA* θ_i in the MSC beam-former.

The choice of the coefficients has to guarantee not only the best suppression of the interfering signals but also the minimization of the expected value of the total output power in order to maintain a low level of white noise.

One drawback of the MSC beam-former is the partial cancellation also of the desired signal that can occur in particular situations: for example it can happen when the desired signal level is very high (compared to the level of the interferences) since it represents a great percentage part of the total output power.

The MSC beam-former is very useful when the desired signal level is very low (compared to the level of the interferences) or when the desired signal itself is absent during well-known time intervals.

6.3.1.1 Experimental results obtained with the MSC beam-forming technique

The capabilities of the MSC beam-forming technique in filtering the interfering signals have been tested on field at the Medicina Radio Astronomical Station.

All the tests have been performed using a channel of the Medicina Radio Telescope Array ("*Northern Cross*") as a primary channel and a broadband omni-directional antenna as auxiliary channel (Figure 6.7).

The receiver installed in the antenna of the *Northern Cross* array works in the bandwidth 400-416 MHz (BEST-1 system, http://www.med.ira.inaf.it/BEST/index_en.htm).

Figure 6.7: A channel of the Medicina *Northern Cross* array used as primary channel (left side) and a broadband omni-directional antenna used as auxiliary channel (right side).

In the first test, an interfering signal continuous wave (CW) has been locally generated at a frequency of 409 MHz and transmitted by a dipole antenna located quite far from the radio telescope. The interfering signal was received with a good signal/noise ratio in both the channels (about 30 dB in the primary channel and 35 dB in the auxiliary channel); the bandwidth of the system (16 MHz @ 408MHz) was down-converted into base-band and filtered by the DDC (Digital Down-Converter).

The MSC filter was designed having 64 coefficients and they were estimated every 400 signal samples. The FFT was applied to the MSC beam-former output signal to plot the results in the frequency domain, it was calculated with 2048 points and every spectrum was the average of 3 spectra in order to reduce the variance of the spectral estimate.

After the processing of the received data, the interfering signal resulted to be completely rejected (Figure 6.8).
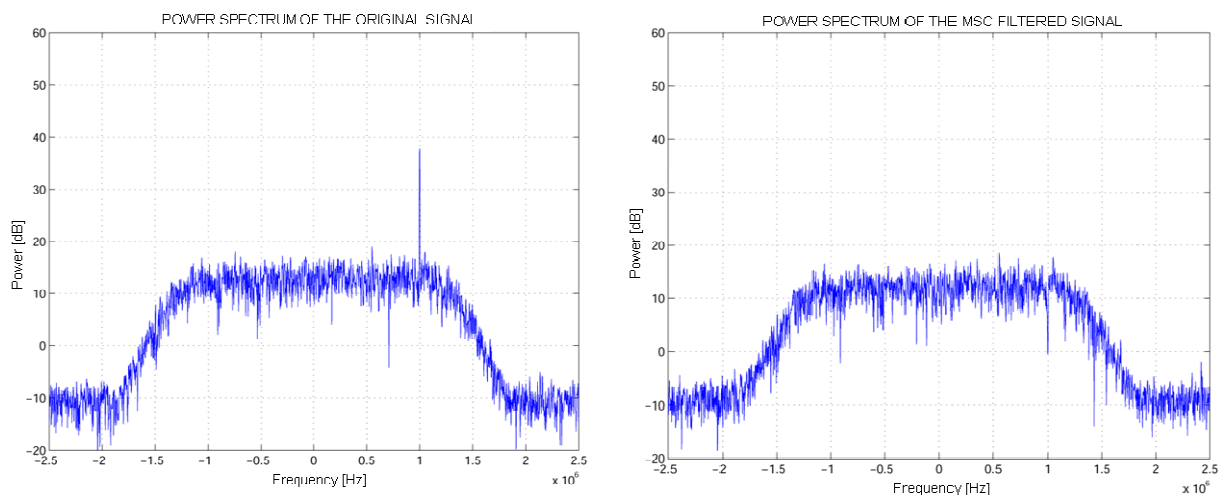
Figure 6.8: Test of the MSC beam-former on a CW interfering signal synthesized at 409 MHz. The interference was completely rejected.

Other tests were carried out on real radio-frequency interferences (not locally generated) whose frequencies are near to the reserved radio astronomical bandwidth.

A digital carrier was detected at 419 MHz and then rejected thanks to the MSC beam-former (Figure 6.9). In this case 32 coefficients, estimated every 100 signal samples, were used to design the MSC filter. Note that the band-pass response of the system is not flat because the system works very near to the cut-off frequency of the filters of the analogue receiver chain.
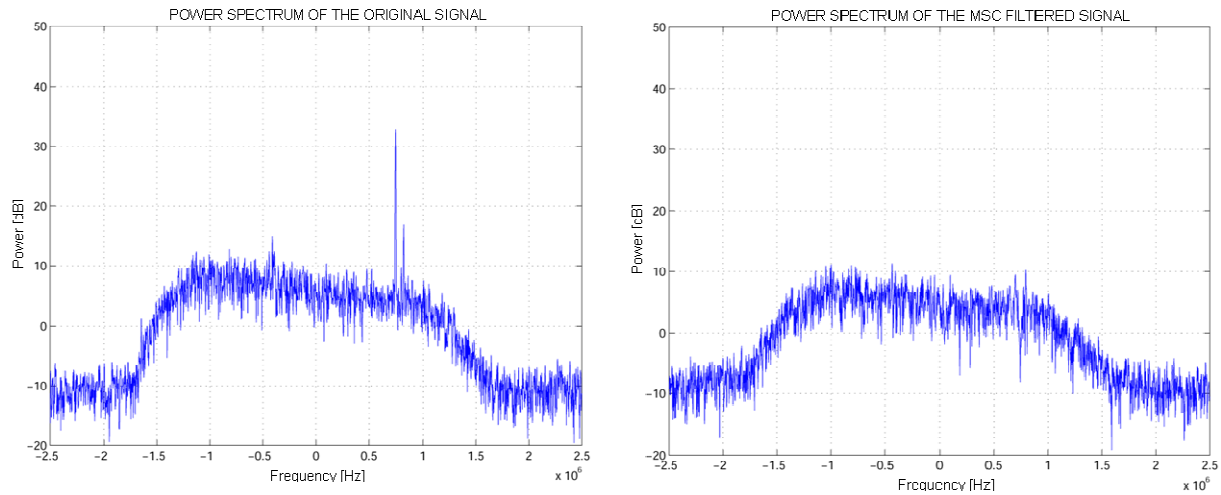
Figure 6.9: Test of the MSC beam-former on a digital carrier at 419 MHz. The interference was completely removed.

An other bandwidth particularly full of interferences is the one around 402 MHz, where there are many telemetry signals. Also in this test satisfying results have been obtained updating quickly the MSC filter coefficients (1 time every 100 samples) and inserting a band-pass filtering at the output of the digital system to mitigate the wideband noise. The attenuation of the interfering signals was of the order of 20 dB (Figure 6.10).
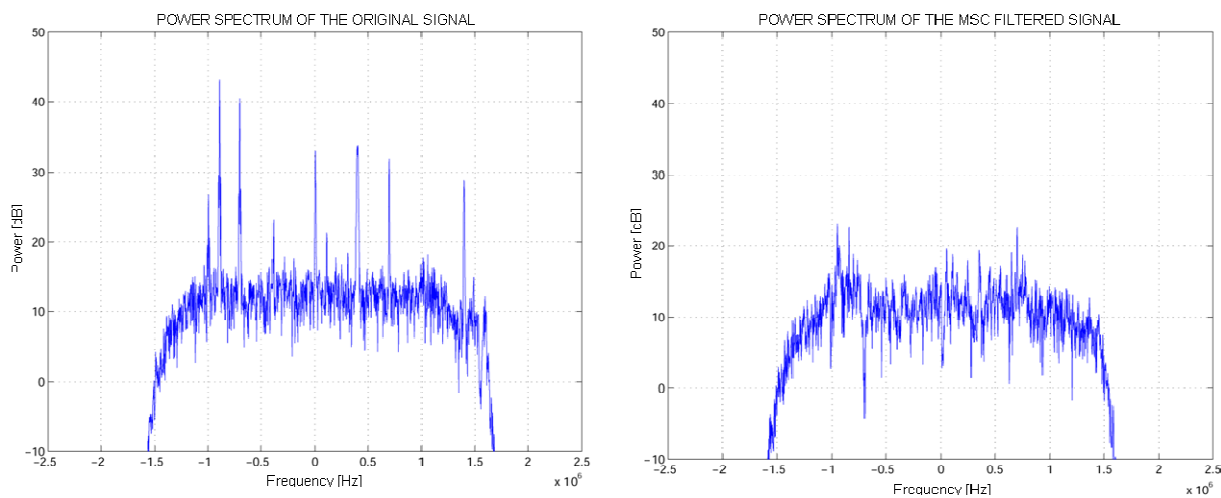
Figure 6.10: The bandwidth around 402 MHz is particularly full of telemetry signals. They have been highly attenuated (about 20 dB).

The last test was performed in order to reject the signals transmitted by a sounding balloon for meteorology at 406 MHz. These sounding balloons are periodically launched from the civil and

military airports and once they are at a high altitude they send down some atmospheric data like temperature, pressure, humidity …

They represent a serious cause of interference for the radio astronomical observations and it can not be easily eliminated. The digital filtering offered by the MSC technique seems to offer a good solution to this problem (Figure 6.11).

As in previous cases, the MSC filter is designed using 32 coefficients estimated every 100 signal samples.
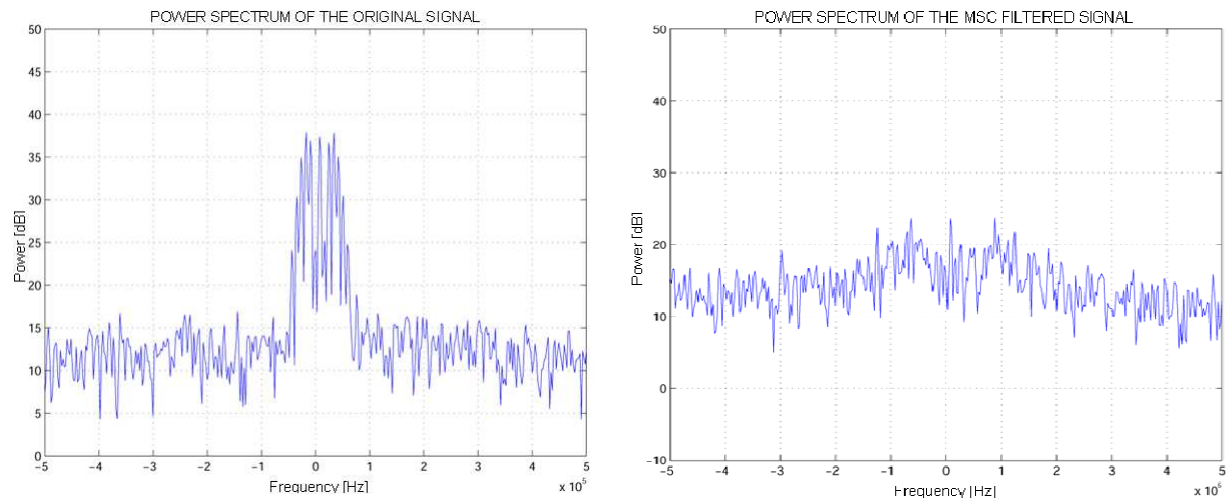
Figure 6.11: Signal transmitted by a sounding balloon for meteorology at 406 MHz. The MSC beam-former offers a valuable solution filtering this signal.

6.3.2. Use of a Reference Signal

If the desired signal was well-known, the coefficients could be chosen in order to minimize the error between the beam-former output and the desired signal itself. The knowledge of the desired signal would make the use of the beam-former useless of course. Nevertheless, in particular applications, the information about the desired signal could be known enough so that it is possible to generate a signal that represents the former one in a good way. This signal is called ***Reference Signal***.

The coefficients are chosen in order to minimize the mean square error between the beam-former output and the reference signal.

The vector of coefficients depends on the cross-covariance between the desired signal component that is in the received signal and the reference signal. Satisfactory performances can be obtained provided that the auto-covariance of the reference signal is close to the desired signal (not known) one. For example, if the desired signal is modulated in amplitude (AM signal), good performances can be usually obtained taking the carrier as reference signal.

Besides, the reference signal is supposed to be uncorrelated with the interfering signals that are in the received signal.

This beam-forming method does not require the knowledge of the *DOA* of the desired signal: this characteristic is an advantage of the method with reference signal.

Simulations showing the performances obtainable using a beam-forming algorithm based on reference signal are presented in [18].

More specifically the beam-former is supposed receiving seven co-channel signals whose main characteristics are summarized in Table 6.1.

Signal	SNR (dB)	Angle (degrees)	Input SINR (dB)
1	24.8	90.0	-13.7
2	14.7	68.0	-24.0
3	18.7	86.9	-20.0
4	10.1	141.0	-28.6
5	18.6	174.3	-20.0
6	38.4	93.2	11.4
7	10.6	26.9	-28.1

Table 6.1: Scenario of the simulation of beam-forming method based on reference signal.

The results of the simulation are summarized in Table 6.2. For comparison, the maximum attainable SINR for each signal is provided.

Signal	Max	Proposed Ref. Signal Beam-forming Method
1	8.5	6.7
2	21.4	16.8
3	7.4	5.5
4	17.0	14.6
5	21.7	17.0
6	28.4	18.8
7	13.5	11.7

Table 6.2: SINR (in dB) of each signal.

Figure 6.12 illustrates the spatial nulling achieved by the proposed beam-forming algorithm based on reference signal. The final weight vectors are used to calculate the gain of the array with respect to the angle of incidence. Dotted radial lines show the angle of incidence of each of the interfering signals listed in Table 6.1. A solid radial line represents the signal of interest.
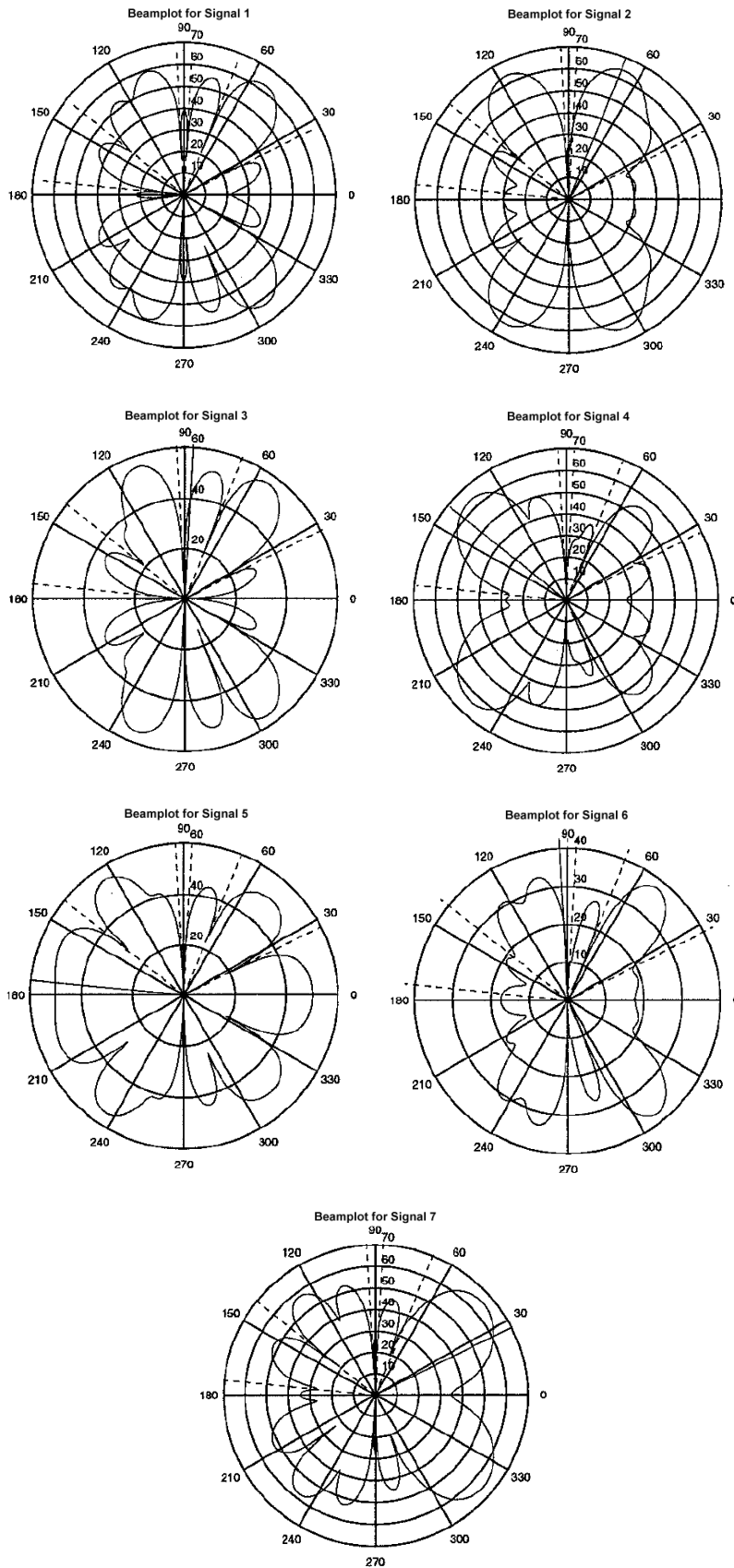
Figure 6.12: Spatial nulling achieved by the proposed beam-forming algorithm based on reference signal. Dotted radial lines show the angle of incidence of each of the interfering signals listed in Table 6.1. A solid radial line represents the signal of interest.

6.3.3. Linearly Constrained Minimum Variance Beam-forming (LCMV)

The **LCMV (Linearly Constrained Minimum Variance)** beam-forming algorithm consists in applying linear constraints to the beam-former response so that the signal(s) of interest can be received with the wanted gains and phases and, at the same time, the possible interfering signal(s) can be canceled out. The beam-former coefficients are chosen in order to minimize the output power (or variance), respecting the constraints. In this way the desired signal(s) is (are) received properly whereas the output contribution due to noise and interfering signal(s) (with different directions of arrival) are minimized.

The use of linear constraints is a general approach that allows an extended control on the adapted response of the beam-former.

With the following linear constraint:

$$\boldsymbol{w}^{H}\boldsymbol{d}\left(\theta,\omega\right)=g \tag{6-6}$$

where g is a complex constant, every signal, coming from a *DOA* θ and having a frequency ω, is certainly received by the beam-former with an output response g.

In order to minimize the contribution due to both noise and interfering signal(s), with frequency ω but not coming from θ, the coefficients are calculated to make the statistical expected value of the output power (or variance):

$$E\left[\left|y\right|^{2}\right]=\boldsymbol{w}^{H}\boldsymbol{R}_{x}\boldsymbol{w} \tag{6-7}$$

minimum.

y is the output of the beam-former and $\boldsymbol{R}_{x}$ is the Auto-Covariance Matrix of the input data.

The LCMV algorithm can be expressed as a minimum search problem, that is:

$$\min_{\boldsymbol{w}} \boldsymbol{w}^{H}\boldsymbol{R}_{x}\boldsymbol{w} \tag{6-8}$$

according to this constraint:

$$\boldsymbol{d}^{H}\left(\theta,\omega\right)\boldsymbol{w}=g^{*} \tag{6-9}$$

To solve this constrained minimum problem, the Lagrange multipliers method can be used, obtaining this fundamental result:

$$\boldsymbol{w}=g^{*}\frac{\boldsymbol{R}_{x}^{-1}\boldsymbol{d}\left(\theta,\omega\right)}{\boldsymbol{d}^{H}\left(\theta,\omega\right)\boldsymbol{R}_{x}^{-1}\boldsymbol{d}\left(\theta,\omega\right)} \tag{6-10}$$

Note: in the real applications the presence of uncorrelated noise ensures that $\boldsymbol{R}_{x}$ can be inverted.

The single linear constraint expressed in (6-9) can be easily extended to the case of more than one linear constraint that allows more control on the array beam-pattern.

For instance, if there is a fixed interference source whose signal arrives from a well-known direction ϕ, whereas the wanted signal arrives from the direction θ (known as well), it could be desirable to force the gain in direction ϕ to *0* maintaining at the same time the beam-former response equal to g in direction θ. This example can be formulated with the following expression:

$$\begin{bmatrix} d^H(\theta,\omega) \\ d^H(\phi,\omega) \end{bmatrix} w = \begin{bmatrix} g^* \\ 0 \end{bmatrix} \qquad (6\text{-}11)$$

If there are $L < N$ (N, the number of the array elements, is also the dimension of the vector space which contains the vectors w and d) linear constraints on w, they can be expressed as:

$$C^H w = f \qquad (6\text{-}12)$$

where the matrix C (with dimension $N \times L$) and the vector f (with dimension L) are called respectively *Matrix of Constraints* and *Response Vector*. The constraints are supposed to be linearly independent, so that C has maximum rank L.

An example of application of the LCMV beam-forming algorithm is reported here following. Only one linear constraint was applied, the one for having the maximum gain toward the direction of the desired signal θ. In other words we have $g=1$ (the gain has been normalized) in equations (6-9) and (6-10). The main parameters of the simulation are summarized in Table 6.3:

Number of array elements	8
DOA of the signal of interest	+10°
DOA of the interference 1	+50°
DOA of the interference 2	-30°
Signal variance	1
Interference variance	10^3
Noise variance	10^{-3}
Central frequency	1.6 GHz
Element spacing	$\lambda/2$

Table 6.3: Parameters used for the simulation of the LCMV beam-forming method

The beam-pattern of the LCMV beam-former has been compared to the one of the classical beam-former with the same conditions (Figure 6.13).
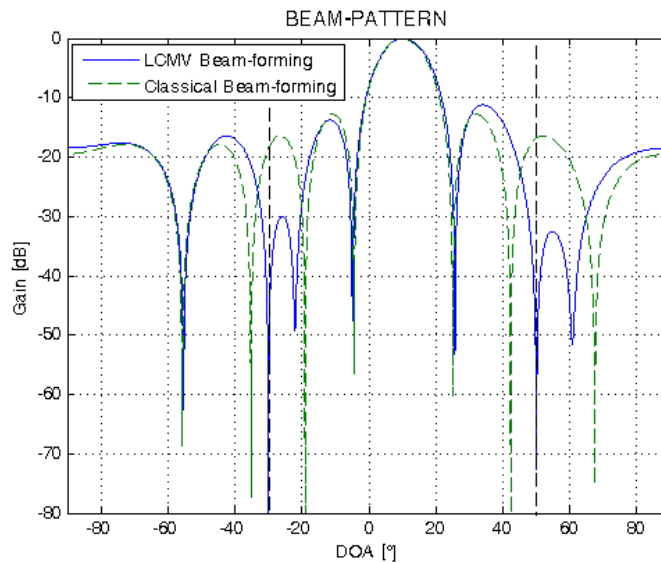

Figure 6.13: Beam-pattern of the LCMV beam-former in presence of a signal with a DOA of +10°, two interfering signals with DOA of +50° and -30° (blue line) and noise. It is compared to the beam-pattern of Classical beam-former, all simulation parameters being the same.

The beam-pattern of the LCMV beam-forming algorithm presents a very low gain (about -70 dB) near the DOA of the interferences: this is achieved thanks to the minimization of the variance of noise and signals not subject to constraints (interferences).

6.3.4. Maximization of the Signal to Noise Ratio (max SNR)

In this method the coefficients are chosen in order to maximize directly the **Signal to Interference and Noise Ratio (SINR)**. A general solution for the calculation of the coefficients requires the knowledge of both the covariance matrix of the signal $\boldsymbol{R}_s$ and the covariance matrix of the noise and interference(s) $\boldsymbol{R}_\eta$. The availability of this a priori information depends on the particular application.

Let's consider the scenario depicted in Figure 6.14. The antenna array receives the signal of interest $s[n]$ that comes from the direction θ and also the noise and interference $\eta_0[n]$. All these signals are sampled and then processed by the beam-former system.
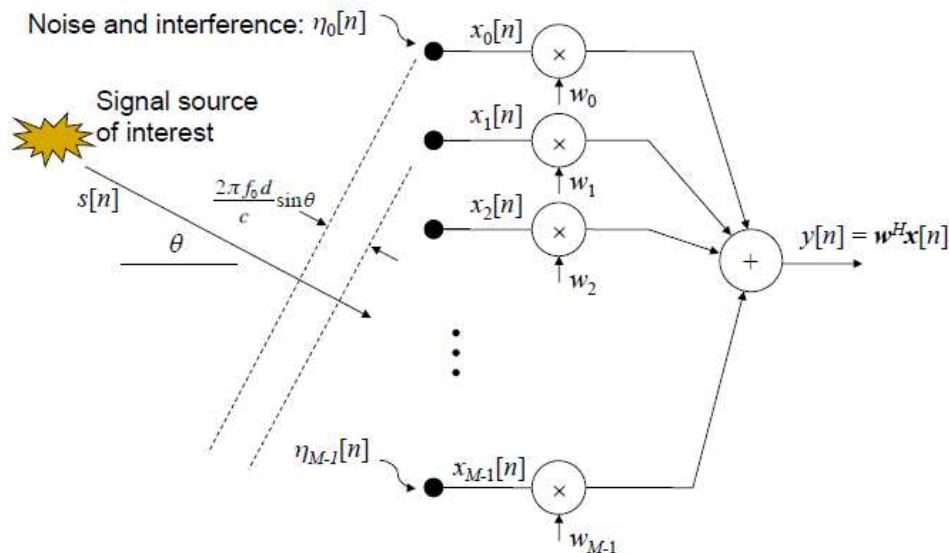
Figure 6.14: Beam-former receiving the signal source of interest in addition to noise and interference.

The sampled array signal contains both the desired and undesired stuff:

$$\boldsymbol{x}[n] = \boldsymbol{s}[n] + \boldsymbol{\eta}[n] \tag{6-13}$$

The SINR at beam-former output is:

$$\frac{E\left\{\left|y_s[n]\right|^2\right\}}{E\left\{\left|y_\eta[n]\right|^2\right\}} = \frac{E\left\{\left|\boldsymbol{w}^H\boldsymbol{s}[n]\right|^2\right\}}{E\left\{\left|\boldsymbol{w}^H\boldsymbol{\eta}[n]\right|^2\right\}} = \frac{E\left\{\boldsymbol{w}^H\boldsymbol{s}[n]\boldsymbol{s}^H[n]\boldsymbol{w}\right\}}{E\left\{\boldsymbol{w}^H\boldsymbol{\eta}[n]\boldsymbol{\eta}^H[n]\boldsymbol{w}\right\}} = \frac{\boldsymbol{w}^H\boldsymbol{R}_s\boldsymbol{w}}{\boldsymbol{w}^H\boldsymbol{R}_\eta\boldsymbol{w}} \tag{6-14}$$

Now if we maximize with respect to $\boldsymbol{w}$:

$$\frac{d}{d\boldsymbol{w}}\left(\frac{\boldsymbol{w}^H \boldsymbol{R}_s \boldsymbol{w}}{\boldsymbol{w}^H \boldsymbol{R}_\eta \boldsymbol{w}}\right) = \frac{2\bar{\boldsymbol{R}}_s \bar{\boldsymbol{w}}\left(\boldsymbol{w}^H \boldsymbol{R}_\eta \boldsymbol{w}\right) - 2\bar{\boldsymbol{R}}_\eta \bar{\boldsymbol{w}}\left(\boldsymbol{w}^H \boldsymbol{R}_s \boldsymbol{w}\right)}{\left(\boldsymbol{w}^H \boldsymbol{R}_\eta \boldsymbol{w}\right)^2} = 0 \qquad (6\text{-}15)$$

we obtain:

$$\boldsymbol{R}_s \boldsymbol{w} = \boldsymbol{R}_\eta \boldsymbol{w}\left(\frac{\boldsymbol{w}^H \boldsymbol{R}_s \boldsymbol{w}}{\boldsymbol{w}^H \boldsymbol{R}_\eta \boldsymbol{w}}\right) \rightarrow \boldsymbol{R}_\eta^{-1} \boldsymbol{R}_s \boldsymbol{w} = \left(\frac{\boldsymbol{w}^H \boldsymbol{R}_s \boldsymbol{w}}{\boldsymbol{w}^H \boldsymbol{R}_\eta \boldsymbol{w}}\right)\boldsymbol{w} \qquad (6\text{-}16)$$

This is a generalized eigenvector equation of the form:

$$\boldsymbol{A}\boldsymbol{w} = \lambda_{\max}\boldsymbol{w}, \ \ where \ \boldsymbol{A} = \boldsymbol{R}_\eta^{-1}\boldsymbol{R}_s, \ \ and \ \ \lambda = \left(\frac{\boldsymbol{w}^H \boldsymbol{R}_s \boldsymbol{w}}{\boldsymbol{w}^H \boldsymbol{R}_\eta \boldsymbol{w}}\right) \qquad (6\text{-}17)$$

Since λ is the SINR, the eigenvector associated with the maximum eigenvalue solves the optimization.

In the case there is a single far field source in spatially white noise, the covariance matrix of the signal $\boldsymbol{R}_s$ and the covariance matrix of the noise and interference(s) $\boldsymbol{R}_\eta$ can be expressed as:

$$\boldsymbol{R}_s = \sigma_s^2 \boldsymbol{d}(\theta_s)\boldsymbol{d}^H(\theta_s), \ \ \boldsymbol{R}_\eta = \sigma_\eta^2 \boldsymbol{I} \qquad (6\text{-}18)$$

where σ_s^2 is the variance (power) of the signal and σ_η^2 is the variance (power) of the noise and interference(s).

The optimal coefficients that guarantee the maximum SNR can be calculated with the following equation:

$$\frac{\sigma_s^2}{\sigma_\eta^2}\left(\boldsymbol{d}(\theta_s)\boldsymbol{d}^H(\theta_s)\right)\boldsymbol{w} = \left(\frac{\sigma_s^2 \boldsymbol{w}^H \boldsymbol{d}(\theta_s)\boldsymbol{d}^H(\theta_s)\boldsymbol{w}}{M\sigma_\eta^2}\right)\boldsymbol{w} \ \rightarrow \ \boldsymbol{w}_{opt} = \boldsymbol{d}(\theta_s), \ \lambda_{\max} = M\frac{\sigma_s^2}{\sigma_\eta^2} \quad (6\text{-}19)$$

Note that in this particular case the solution is the same as the classical beam-former one.

An example of the results achievable with the Max SNR beam-forming method is presented in Figure 6.15. It refers to the simulation parameters of Table 6.4.

Number of array elements	10
DOA of the signal of interest	+20°
DOA of the interference	-10°
Signal variance	1
Interference variance	10^3
Noise variance	10^{-4}
Central frequency	1.6 GHz
Element spacing	$\lambda/2$

Table 6.4: Parameters used for the simulation of the Max SNR beam-forming method

The application of the Max SNR beam-former in presence of a single interferer plus i.i.d. (independent and identically distributed) noise has been compared to the case with no interferer (only i.i.d. noise) and also to the case of application of the classical beam-former with Kaiser windowing.

The results of the simulation are the following:

- Classical beam-former, with interferer at -10°, SINR = +3.20;

- Max SNR beam-former with no interferer, SNR = +50;

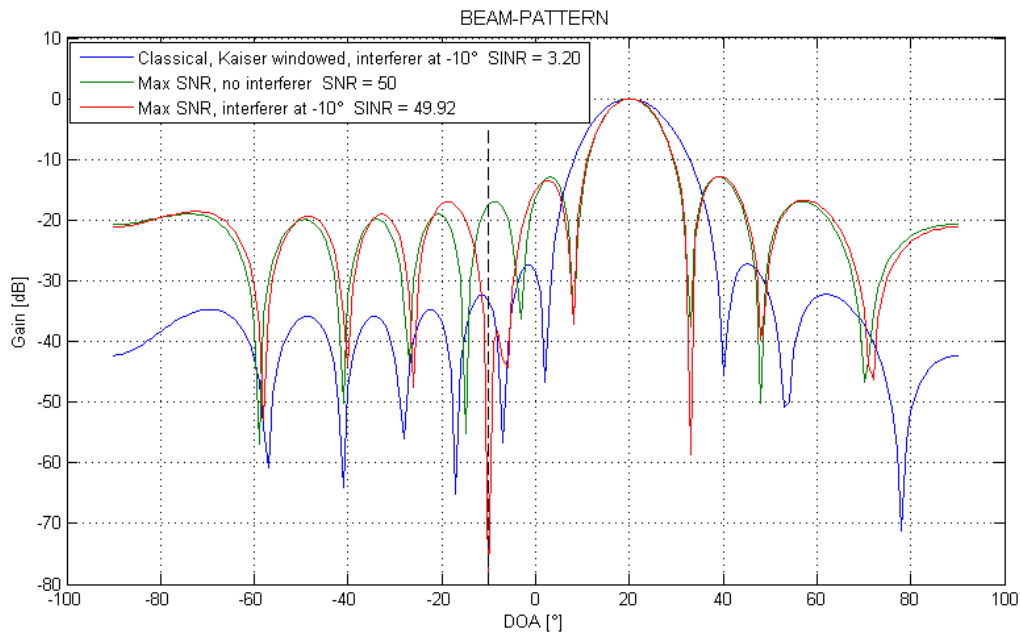- Max SNR beam-former with interferer at -10°, SINR = +49.92.

Figure 6.15: Beam-pattern of the Max SNR beam-former in presence of a signal with a DOA of +20°, an interfering signal with a DOA of -10° (red line) an d i.i.d. noise. It is compared to the beam-pattern of Max SNR beam-former for the case with no interferer (green line) and with the one of classical beam-former (blue line).

7. Conclusion

The design of a multi-band antenna system suitable to provide to a mobile phone device the functionality in GNSS (1572.42 MHz), GSM/GPRS/UMTS (1800/1900/2100 MHz) and Bluetooth/Wi-Fi (2400 MHz) bandwidths is not a trivial activity at all.

The handset designer faces several problems when incorporating multiple antennas (multiple bandwidths) on the same PCB. First, they have to be very low cost (a few cents, probably). Secondly, they have to be broadly omni-directional, since the signals can arrive from whatever direction. Moreover from the GNSS receiver point of view, we would like the antenna to be as far from the communications (transmitting) antenna as possible, and also removed from other transmitting services such as Bluetooth, Wi-Fi, and, if present, FM. Users must not be able to detune the antenna out of band by placing their hands on the phone, or by raising the phone to their ears. So the antenna designer has to face several important problems.

Preliminary antenna design results have been obtained for a mobile device with GPS, GSM1800, UMTS and WLAN/Bluetooth capabilities.

Acceptable radiation patterns, reflection coefficients and isolations have been achieved using very basic and cheap antennas in a combined-radiator architecture.

These results provide a good starting point for the development of high performance devices.